MgAl層状複水酸化物を用いた水溶液からのホウ素の除去

Alkhudhayri, Abdulrahman S Sami
九州大学大学院総合理工学府大気海洋環境システム学専攻

令和元年度
九州大学大学院総合理工学府
大気海洋環境システム学専攻修士論文

Removal of boron from aqueous solutions using MgAl Layered Double Hydroxide

[MgAl 層状複水酸化物を用いた水溶液からのホウ素の除去]

氏　　名
Sami Abdulrahman S Alkhudhayri

指導教員名
Osama Eljamal

Acknowledgement

All praise and thanks is due to Allah, the lord of mankind and all that exists, for his blessings, benevolence, and guidance at every stage of our lives.

I would like to dedicate this work to my parents, brothers and sisters for their continuous support and unconditional love.

Sincere gratitude to my supervisor Professor Osama Eljamal for his guidance throughout my Masters study.

I also appreciate the critical reviews and assistance of my colleagues in the Environmental Fluid Science Lab (EFSL) regarding my progress.

Finally, I extend my deepest appreciation to my country the Kingdom of Saudi Arabia for providing me with this great opportunity

Table of Contents

List of Tables

Table of Figures

Abstract

Although boron, in controlled amounts, is an element of requirement for the growth of plants, animals and humans, environmental issues and health hazards are related to boron applications in various industries. For many countries that suffer from the lack of natural water resources like the Kingdom of Saudi Arabia, United Arab Emirates, and Kuwait; seawater desalination plants such as, reverse osmoses (RO) plants are vastly implemented. Boron rejection percentage using RO distillation is too low considering drinking water regulations in those countries. Recently many techniques have been developed to remove boron from aqueous solutions; adsorption proved to be capable to treat solutions with low boron concentrations. In this study, Mg-Al layered double hydroxide (LDH) was successfully synthesized and calcined. The synthesized LDH was tested in a process to remove boron from aqueous solutions. Experiments were conducted with various parameters of reaction conditions in removing the contaminant from aqueous solutions, such as pH values, operating temperatures, various boron initial concentrations, amounts of Mg-Al-LDH dosages, aerobic conditions, and anaerobic conditions, to determine the optimum operating factors in the removal of boron from aqueous solutions using Mg-Al-LDH. Scanning Electro-Microscopy (SEM), Transmission Electro-Microscopy (TEM), and X-Ray Diffraction (XRD) analyses were conducted to study the characteristics of the sorbent. Furthermore, kinetics, isotherm, and thermodynamic modeling were considered to determine Mg-Al-LDH sorption method.

Some of the core findings in this study included that the sorption kinetic rate got higher by approaching towards the neutral pH conditions, while it declined at the strong acidic or alkaline conditions. Moreover, higher removal rates of boron in aqueous solutions were observed at increased temperatures reflecting the endothermic nature of the reaction, and at temperature 70 ℃ it reached equilibrium at less than 6 hours. Furthermore, isotherm modeling confirmed that boron removal by Mg-Al-LDH occurred through a mono-layer sorption, and thermodynamic modeling revealed the positive value of entropy change indicating that the randomness of the solid/liquid interaction increases within the adsorption process of Boron

Keywords: Boron, Mg-Al-LDH, Seawater, Isotherm Modeling, Kinetics, Thermodynamic Modeling.

1. Introduction

Boron (B) present in nature is a natural phenomenon and found in forms of boric acids (H_3BO_3) and borate salts in small amount, though most of the boron found in water bodies, surface water and groundwater, are most likely the result of manmade pollution [1]. Boron found in surface water is a result of wastewater discharge with high amounts of detergents which contain borate (BO_3). Moreover, industrial discharge from glass, film, food preservatives and fertilizers hold major part in water pollution by boron [1], [2]. Whereas, the boron found in groundwater in the form of borate and borosilicate are mainly the aftermath of leaching from sedimentary rocks and some soils [3]. Boron concentrations range from <0.3 to >100 mg/L in groundwater worldwide, moreover in surface water where the majority of boron is located at an average concentration of 4.5 mg/L [4]. The estimated average consumption of boron in daily dietary was determined to be at 1.21 mg/day for food and 0.2~0.6 mg/day for drinks [5]. Boron is necessary for plants only in controlled amounts depending on the different types of plants otherwise there might be severe side effects such as retardation of growth. Meanwhile, humans' nerve system as well as reproductive system are also effected by consumption of large amounts of boron [6]. World Health Organization (WHO) has established guidelines for boron's concentration in drinking water to be 0.5 mg/L [7]. For many countries with large arid and semi-arid surfaces that suffers from the lack of natural water resources; such as the Kingdom of Saudi Arabia (KSA), United Arab Emirates (UAE), and Kuwait. KSA is well known for having the world's largest desalination plants standing at about 30 plants, with variety of desalination approaches including Multi-stage, Multi-effect and Reverse Osmosis (RO) [8], [9]. RO plants are efficient and environmentally friendly, but when it comes to removal of seawater elements and salts it fails to remove the boron completely. Although it is easy for RO membranes to separate negatively charged borate ion (BO_3^{2-}) from contaminated water, removing neutrally charged boric acid found in sea water is in fact difficult to achieve. It has been reported that removal rates using RO membranes vary depending on the treatment pH range; boric acid recorded rejection rates of 40-60% at pH range of 5.5-9.5, on the other hand, in the same pH conditions borate ion registered removal rates at 95% [10].

Many mechanisms were considered for the removal of boron in aqueous solutions; such as adsorption, reverse osmosis (RO), ion exchange, electrocoagulation, Donnan dialysis, chemical coagulation, hybrid process[11]–[13]. Various sorbents have been tested for their adsorption capabilities in regards to boron removal; such as activated carbon [14], fly ash, clays, natural minerals, LDHs, biological

materials [15], oxides [16], mesoporous silica, nanoparticles, complexing membranes [17] and selective resins [18]. One of the promising and most effective methods is adsorption process using LDH or LDH-like materials [19]. LDH-like compounds, also referred to as Hydrotalcite, are a type of layered materials with the general chemical composition of $[M^{2+}_{1-x}M^{3+}_{x}(OH)_2]$ $(A^{n-})_{x/n}\cdot mH_2O]$, M^{2+} is divalent cation and M^{3+} is trivalent cation, A^{n-} is an interlayer anion with charge n, and x is the $[M^{3+}]/([M^{2+}]+[M^{3+}])$ molar fraction [20]–[22]. Considering brucite $[Mg(OH)_2]$, LDH's structure can be described as infinite sheets connected by sharing edges as octahedral magnesium oxide (MgO_6). Once the divalent cations were to be replaced with trivalent cations, the sheets become positively charged. Instantaneously, fitting sum of anions become inherent in the hydrated interlayer galleries to stabilize the positive charge [23]. Having a flexible composition is LDH's most favorable advantage; altering of its divalent and trivalent ions' characteristics, atomic ratio and the wide range of altering the nature of the interlayer without changing its basic structure. Thus, LDHs are applicable in various fields as, catalysts or catalysts precursors, anion exchangers, flame retardants, stabilizers for polymers and electroactive/photoactive materials [24]–[26]. Many types of LDHs, classified by the type of the merged cations in LDH layers, have been considered in water treatment applications [27]. Nevertheless, few of those LDHs were reported to have been utilized to the removal of boron in aqueous solutions. Mg-Al-LDH has been tested and reported to have unique properties such as high adsorption capacity, exceptional anion exchange rate and mobility of interlayer anions in water molecules [28].

It has been reported that boron adsorption capacity on Mg-Al-LDH is greatly enhanced once the LDH is calcined at high temperatures. As calcination changes the structure of Mg-Al-LDH's interlayer and metal oxides, leading to an increased intake capacity of boron on the LDH. Delazare et al. [29] stated that the calcined Mg-Al-LDH had higher sorption capacity than that of the uncalcined Mg-Al-LDH when used to treat borate tainted oilfield wastewater. Furthermore, they pointed that the optimum pH for the removal of both contaminants varied between 9.0-9.2. Kentjono et al. [30] used Mg-Al-LDH on the removal of boron and iodine similarly by treating optoelectronic wastewater contaminated boron and iodine at high concentrations; where LDH showed efficient removal of both contaminants, though boron had more affinity to be adsorbed by the LDH where the maximum boron uptake capacity was observed at pH of 9.0, when only less than 50% of boron is in the tetrahydroxyborate ($B(OH)_4^-$) form.

Many researchers have investigated Mg-Al-LDH on boron removal but only in precise aspects separately like pH and temperature effects. In that regard, the main objective of this paper is to

consider more parameters to be investigated at the same time to reach a concrete conclusion regarding the removal capabilities of Mg-AL-LDH towards boron removal. The effect of different parameters has been investigated on the removal process, including pH levels, temperatures, initial boron concentrations, dosage amounts, aerobic and anaerobic conditions. Moreover, morphology and crystallinity characteristics have been examined for the solid samples using transmission and scanning electron microscopies (TEM), (SEM), as well as X-ray diffraction (XRD), respectively. Deepen insights into the removal mechanism of boron by Mg-Al-LDH were determined considering detailed kinetic, isotherm and thermodynamics analyses.

2. Materials and Methods

2.1. Materials

The hydrotalcite-like material Mg-Al-LDH was synthesized using the following materials magnesium nitrate hexahydrate ($Mg(NO_3)_2.6H_2O$), aluminum nitrate nonahydrate ($Al(NO_3)_3.9H_2O$), and sodium hydroxide (NaOH) [31]. Stock solution of 500 mg/L initial boron concentration was prepared using boric acid (H_3BO_3). Diluted hydrochloric acid (HCl) and concentrated sulfuric acid (H_2SO_4) were considered for pH adjustment and boron concentration analysis, respectively. All solutions were prepared using deoxygenated deionized water.

2.2. Mg-Al-LDH's Synthesis

The preparation of 10 g Mg-Al-LDH was carried out in the duration of three days; 700 mL aqueous solution containing 0.1 mmol (25.6406 g) of $Mg(NO_3)_2.6H_2O$ and 0.05 mmol (18.7565 g) of $Al(NO_3)_3.9H_2O$ were mixed vigorously [30]. The solution mixture was then added drop wise to 1500 mL of 2 M NaOH solution while stirred using a mechanical mixer set at 400 rpm. The temperature was kept at 45±3℃ during the process. Slurry obtained was then heated for 2 hours (T=85±3℃) under slow mixing at 200 rpm. The solution was kept in room temperature for 12 h. Next day; The slurry product was separated by centrifugation technique and washed with deionized water several times until pH reached 8.5-9.5 and conductivity was constant. The solids were dried at 60℃ for 48h. Then, small part of the dried product was collected for further use as uncalcined LDH, while the rest was calcined at 550℃ for 4 h. The solids were dry and light enough to be crushed into powder-like form which were later kept in a concealed container for the batch experimental use. Abbas et al. [16] have reported that sorption of boron on magnesium oxide and aluminum oxide reached its maximum sorption capabilities at pH 9.5, and pH 8, respectively, which was the reason why the sorbent's pH was determined to be pH 8.5-9.5 during synthesis.

2.3. Characterization and Chemical Analysis

The physical characteristics of Mg-Al-LDH composites were investigated by several equipment. The surface morphology was investigated using a transmission electron microscopy (TEM, JEM-2100F, JEOL Co., Japan). Scanning electron microscopic analysis was conducted using (SEM, JCM-6000, JEOL Co., Japan) coupled with energy dispersive X-ray spectrometer (EDS) for the determination of the shape and size of the synthesized particles. Mineral composition of Mg-Al-LDH was determined

by X-ray diffraction (XRD) analysis, using Cu Kα radiation (λ = 1.5418 Å) on TTR Rigaku diffractometer set at 40 kV and 40 mA, with scanning angle (2θ), ranged from 3° to 90° and scanning speed of 2° min−1 [32].

Using the HACH-DR3900 UV-vis spectrophotometer, the following process was commenced for boron concentration analysis: 75 mL of sulfuric acid in a 400 mL conical flask. One bag of BoroVer 3 Boron Reagent Powder was added and mixed well for 5 minutes. 35 mL of the above mixed reagent was added to another two flasks. 2 mL of deionized water was added to one flask and another 2 mL of the boron contaminated water was added to the other flask, then mixed well. After 25 minutes of reaction time, the solutions were added to measuring vials and wiped of any excesses, then measurement was conducted.

2.4. Batch experiments

The experiments were conducted to investigate the sorption of boron on Mg-Al-LDH using only polypropylene (PP) flasks, in order to avoid reaction of boron with glass. all the basic value of the parameters, to be considered in the patch experiments, were determined based on a previously performed optimization with respect to the highest removal efficiency towards boron. Solution volume of 100 mL, with the following basic operating conditions; pH = 9, temperature of 25℃, boron initial concentration of 20 mg/L, and Mg-Al-LDH dosage of 2 g/L. To further investigate variations of mentioned parameters a study of their effects on the removal of boron. pH effect on the removal of boron on Mg-Al-LDH different pH levels (3, 6, 9, and 12) were considered. Temperature effect was also examined with a range of (25, 40, 55, and 70 ℃). Effects of boron initial concentrations were examined as well (5,10, 20, 40, and 80 mg/L), and LDH dosages of (0.1, 1, 2, 5 g/L) were studied as well. Furthermore, to study anaerobic and aerobic conditions two separate experiments were conducted; the anaerobic test was done using nitrogen purging during the whole time of the experiment to provide anoxic environment, and aerobic test was conducted by pumping air into the batch throughout the whole experiment as well. Thus, enabling us to find the best conditions for the optimum sorption capacity to take place.

In order to simulate the real conditions of boron removal from real seawater, synthesized seawater was considered as batch solution. Based on the ASTM standard practice for preparing ocean water (D 1141 – 98 (2003)) [33]. Components used for seawater synthesis are as in (Table 1) were added to 1 L of deoxygenated deionized water in a polypropylene flask, and kept as a stock solution.

Comparison were conducted on the removal of boron between the synthesized boron solution and the synthesized seawater solution with boron concentration of 5 mg/L. Samples of 5 mL were withdrawn at specific time intervals during 24 h, then analyzed for boron concentration.

NaCl*	$MgCl_2.6H_2O$*	Na_2SO_4*	$CaCl_2$**	KCl*	$NaHCO_3$*	H_3BO_3**	$SrCl_2$*
24.53g	5.20g	4.09g	1.16g	0.695g	0.201g	0.027g	0.025g

*FUJIFILM Wako Pure Chemicals – Japan.

**JUNSEI – Japan.

Table 1 seawater synthesis

3. Results and Discussion

3.1. Characterization

For characterization of Mg-Al-LDH three equipment were used; transmission electron microscopy (TEM), scanning electron microscopic (SEM), and X-ray diffraction (XRD).

3.1.1. TEM analysis

The TEM device demonstrated the shape and size of freshly synthesized Mg-Al-LDH, as shown in Fig. 01. The shape of the sorbent can be described as micro integrated hexagonal and octahedral plate particles, and inhomogeneous particles. The sizes of those particles varied in the range of 40-100 µm. Moreover, morphology investigation revealed the particles network with a clear interlayer effect.

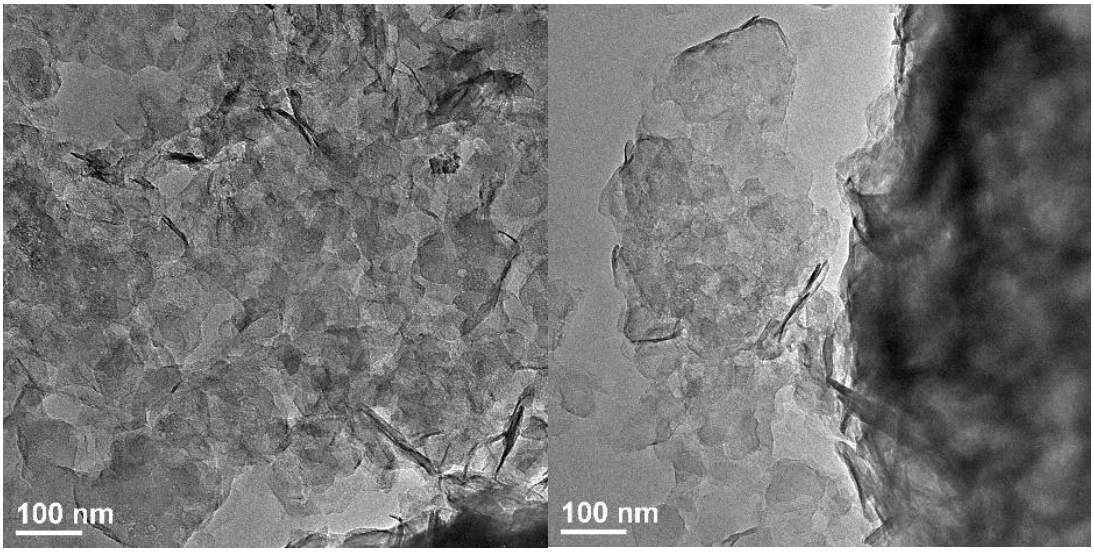

Figure 1 TEM analysis of freshly synthesized Mg-Al-LDH.

3.1.2. SEM analysis

The elemental mapping and EDS spectrum of the SEM images taken for spent Mg-Al-LDH are shown in Fig. 02. The elemental mapping revealed the well morphological distribution of Mg and Al elements, which was associated with the sorption of boron on the surface of the composite. Such results were confirmed by the presence of boron peak within the EDS spectrum with content ratio of 2.45%.

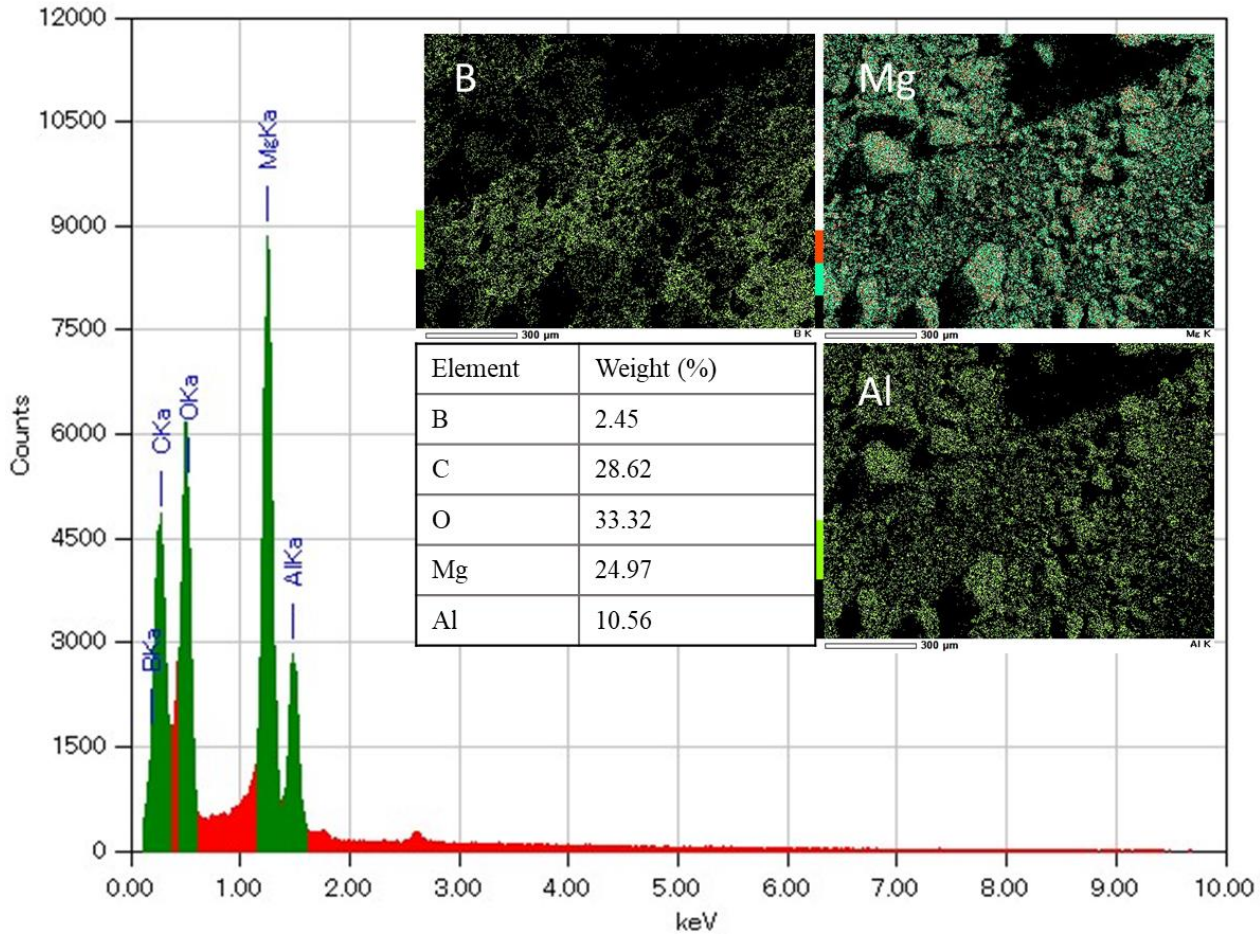

Element	Weight (%)
B	2.45
C	28.62
O	33.32
Mg	24.97
Al	10.56

Figure 2 SEM/EDS analysis of a spent sample's solid residual

3.1.3. XRD analysis

Analysis of two Mg-Al-LDH samples were used in order to visibly prove the adsorption of boron on Mg-Al-LDH. Fig. 03 analysis of a freshly synthesized sample (a) and solid residues of a spent pH 9 experiment (b) is shown. The pattern of the fresh sample represents a successful synthesis of Mg-Al-LDH with clear Mg-Al-O complexes corresponding to XRD peaks at 2-thetas of 43.154°, and 62.633°. Moreover, magnesium oxide (MgO) peak appeared at 2-thetas of 35.21°, which was attributed to the excess magnesium within the system, as it has been previously reported [34], [35]. Whereas the spent sample demonstrates an observed boron sorption on Mg-Al-LDH; corresponding to sharp peaks associated with the Mg-Al-B formed compounds on the hydrotalcite surface at 2-thetas of 11.198°, 22.6°, 35.4°, 47.2°, and 62.3°. Additionally, the presence of boric acid ($B(OH)_3$), as one of the dominant boron species, was confirmed in the spent sample by interfered peaks. The peaks of Mg-Al-LDH in the fresh sample were either disappeared or substituted by B-complexes peaks in the spent one. Although the graph illustrates broad peaks in the freshly synthesized sample analysis, the sharp peaks shown could be an indicator that the synthesized-calcined Mg-Al-LDH is of semi-crystalline structure.

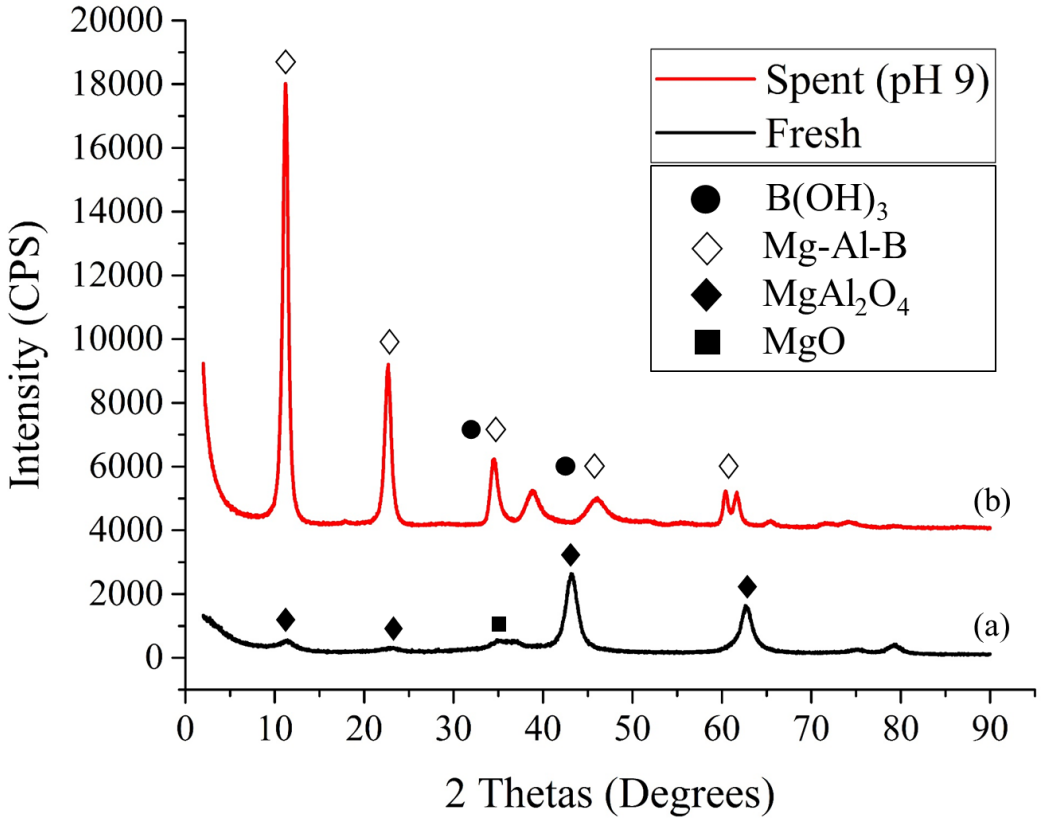

Figure 3 XRD patterns comparison of freshly synthesized Mg-Al-LDH and spent samples

3.2. pH Effects

After testing pH levels (3, 6, 9, and 12) at different initial boron concentrations (5, 10, 20 mg/L) pH 12 showed the least removal rate of boron throughout the entire mixing process, whereas the other pH values showed much better performance. As shown in Fig. 04, pH 9 had the most rapid removal rate to reach boron concentration of 7.2 mg/L after only 1 h from the beginning of the experiment. It is worth mentioning that pH 3 and 6 showed a comparable performance to pH 9 with an almost identical trend. Nevertheless, pH 9 was slightly superior with the lowest boron equilibrium concentration of 0.2 mg/L after 24 h reaction time. In other experiments (data are not shown), considering lower initial concentrations (5 and 10 mg/L), pH 12 showed the same lowest removal rate, followed by pH 3.

This phenomena could be explained with the change of boron species in aqueous solutions under different pH, where in pH 0-9 Boric acid (H_3BO_3) is the dominant species and in pH 9.5-13 tetrahydroxyborate $B(OH)_4^-$ species are dominant. Considering magnesium oxide ($Mg\text{-}O_3$) ions' surface are positively charged in pH 0-11.9 (point of zero charge (PZC) = pH 12), and aluminum oxide ($Al\text{-}O_3$) positive charge is pH 9 and under [16]. We can deduce that negatively charged boron species are strongly withdrawn by the Mg-Al-LDH at its concentrated positively charged ions which occur in pH 5-9.6, where both oxides are working at their highest removal rate in accordance to temperature. When pH level is at pH 12 $Al\text{-}O_3$ ions are at a negative charge, leading to repel the negatively charged $B(OH)_4^-$ ions and only close to PZC $Mg\text{-}O_3$ are adsorbing boron species found in the solution; which is higher than can be adsorbed.

Such results implied that strong acidic or alkaline conditions are not so preferable for boron removal by Mg-Al-LDH. That implications will be confirmed later be detailed kinetic analysis and the proposed removal mechanisms corresponding to the pH conditions and available aqueous boron species. From the previously discussed results, it is concluded that the removal of boron species from aqueous solutions onto Mg-Al-LDH is dependent on the solutions initial pH 5-9.6 values. Qiu et al [36] reported similar results in accordance of pH effects on the sorption of boron onto D-LDH-700 but the dosage (2.5 g/L) which is higher of that conducted in this study, though maximum sorption capacity in this study was higher by 22.01 mg/g compared to theirs which was 2.37 mg/g.

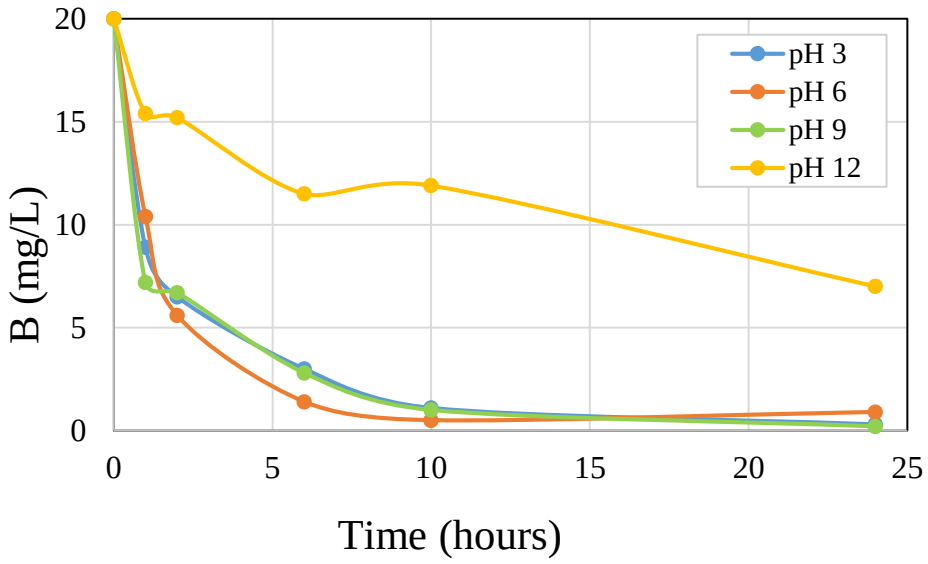

Figure 4 pH level effect on the enhancement of boron adsorption on Mg-Al LDH, (experimental conditions: initial concentration = 20 mg/L, 25 ^{o}C and Mg-Al-LDH dosage of 2 g/L)

Residual solids from pH 3 (a) and pH 9 (b) experiments were collected and analyzed using XRD analyzer to confirm which is the optimum pH by comparing the boron intensity found in those samples. Fig.05 illustrates similar patterns of both samples with an only difference in intensity count. Sample pH 3 showed high sorption of boron onto Mg-Al-LDH by displaying intensity values of 15397 cps in the first peak at 2-thetas 11.19° and 5718 cps in the second peak at 2-thetas 22.6°. Whereas, sample pH 9 recorded boron species (Mg-Al-B) intensity of 18669 cps at 2-thetas 11.19° and 6724 cps at 2-thetas 22.6°. Nevertheless, results collected form batch experiment conducted to test the effects of pH on the removal of boron by adsorption on calcined Mg-Al-LDH, proved that pH 9 hold the higher boron removal compared to that of pH 3.

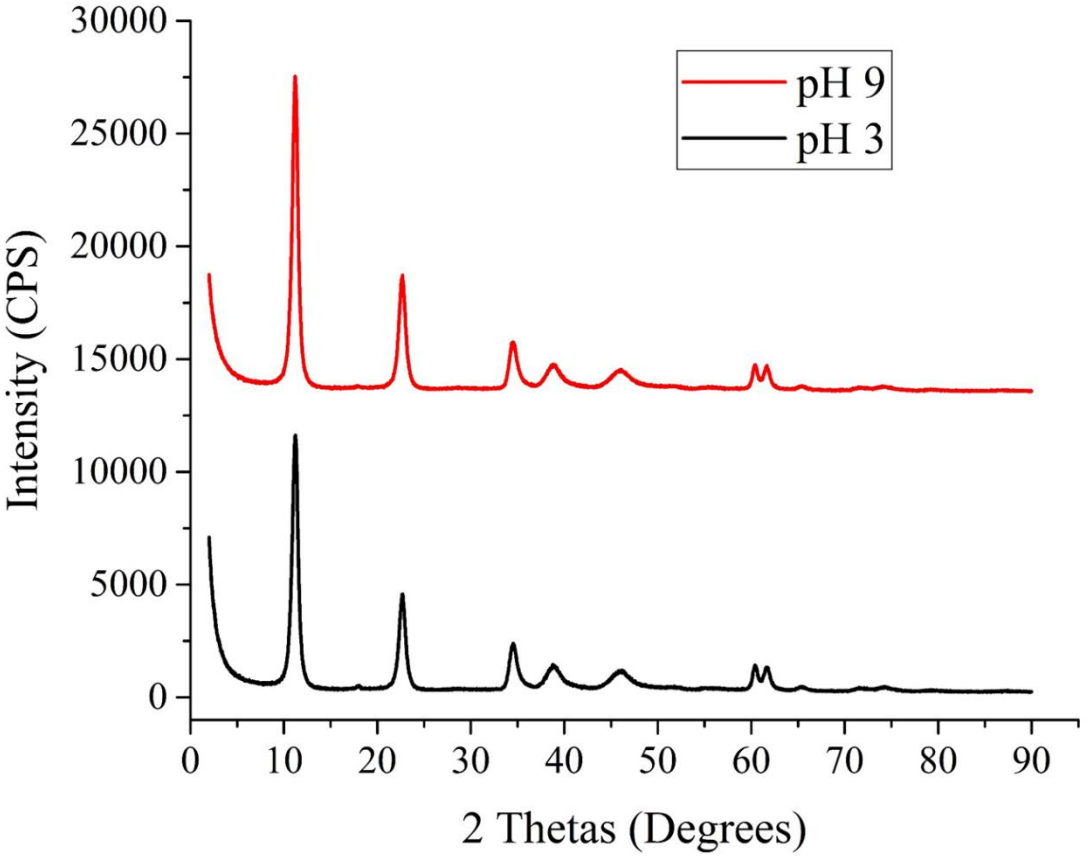

Figure 5 XRD pattern comparison between pH 3 and pH 9 solid residuals

3.3. Temperature Effects

In this experiment temperatures that of an average room temperature to that of industrial levels were examined to further understand the sorption mechanism of boron on Mg-Al-LDH. Where the analysis of the samples taken over the set time intervals dictated that with increased temperatures higher removal rates of boron in aqueous solutions were observed. as shown in the Fig. 06 at temperature 70 ℃ reached equilibrium at less than 6 hours with higher removal rate than that of the other temperatures which have not reached the same sorption value even after 24 hours of reaction time. Such results reflected the endothermic nature of the removal process of boron by Mg-Al-LDH, where the higher temperature introduced to the reaction the better the removal efficiency is achieved.

Isaacs et al [37] reported that with increased temperature (up to 35 °C), sorption capacity of boron onto Mg-Al-LDH has decreased; compared to lower temperatures such as 15, 25 °C where both temperatures showed similar adsorption capacities. Unlike this study where in order not to have temperatures close to that of an average room temperature, that could lead to similar results as to what have been reported by them. Temperatures higher than 35 °C were chosen and tested and resulted with opposite adsorption capacities than to what have been reported as well.

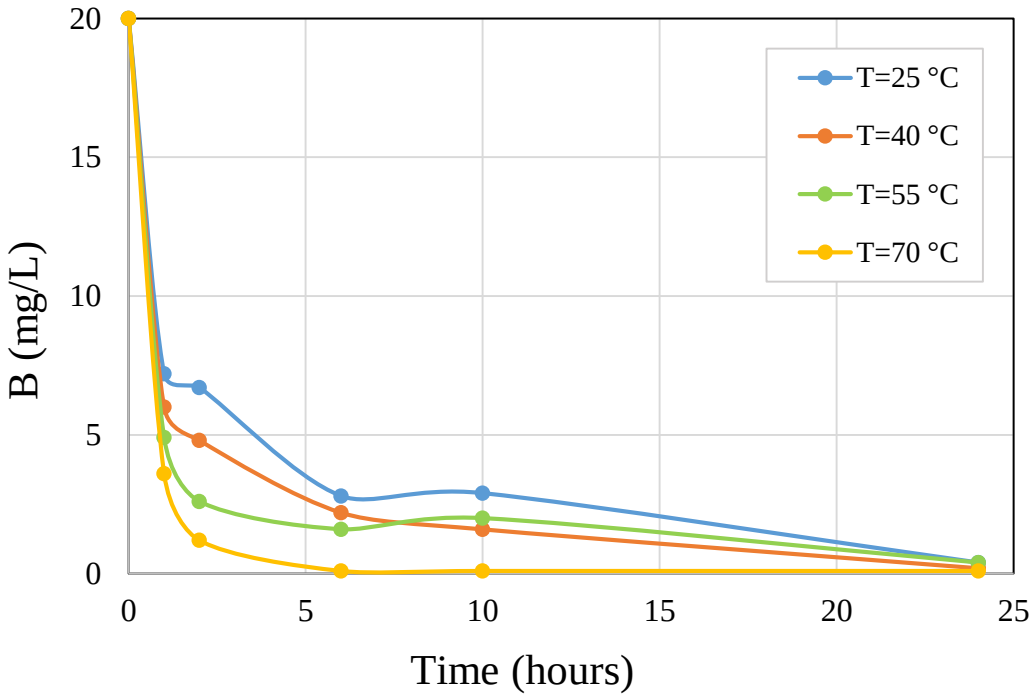

Figure 6 temperature effect on the enhancement of boron adsorption on Mg-Al LDH, (experimental conditions: initial concentration = 20 mg/L, pH = 9 and Mg-Al-LDH dosage of 2 g/L)

3.4. Concentration Effects

Even with high concentrations of boron, Mg-Al-LDH proved to be an efficient sorbent to boron contaminate solutions. Fig. 07 indicates that up to the point of boron initial concentration of 40 mg/L with only 2 g/L of Mg-Al-LDH; the removal of the contaminant is at a clear inclined pace and reaching equilibrium in some cases. With the same dosage at initial concentration of 80 mg/L have shown promising results in the removal of the contaminant the first 18 hours of the experiment, but clear desorption is detected. That can be explained by discussing the two main aspects of this experiment; when the concentrations were lower (5, 10, 20 mg/L), boron species were already low and they have been adsorbed onto Mg-Al-LDH without reaching its maximum sorption capacity. While in the case of initial concentration 40 mg/L, boron reached to lower stage than its starting point and the surface area of the adsorbent is not fully occupied. For the highest initial concentration 80 mg/L; though large amount was being adsorbed into the LDH. With time, the sorption capacity is lowered due to the surface sites' full occupation to the point that there are still boron species left in the solution. Moreover, desorption is possible to occur at high boron concentrations which was confirmed by the sudden rise in case of 80 mg/L to reach 36.1 mg/L after 24 h from the beginning of the reaction. In conclusion, boron removal by Mg-Al-LDH seemed to be initial concentration independent at low concentration levels, while it has a significant effect at high initial concentrations.

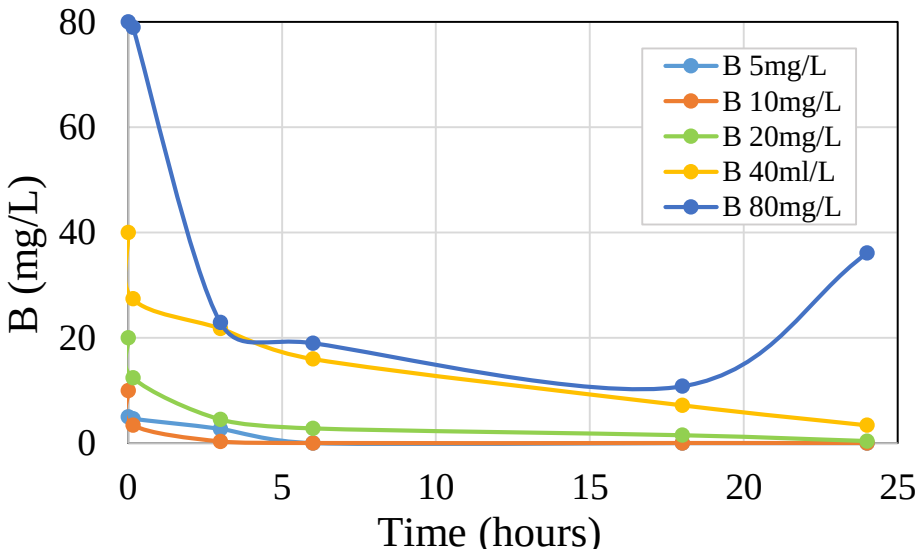

Figure 7 Concentration effect on the enhancement of boron adsorption on Mg-Al LDH, (experimental conditions: pH =9, 25 ºC and Mg-Al-LDH dosage of 2 g/L)

3.5. Dosage Effects

The higher the Mg-Al-LDH dosage is the higher the sorption of contaminant is. Fig. 08 illustrates different Mg-Al-LDH dosages and their removal trends on boron initial concentration of 20 mg/L. With increased dosages higher removal rates are observed, even with dosage value of 1 g/L removal rate is very clear though, it reached its maximum adsorption at 8 mg/L of boron concentration. The trend for dosage value of 2 g/L shows slight desorption due to sorption capacity weakening by high boron species compared to LDH dosage amount. The trend of both dosages 2 and 5 g/L are similar to each other, where 5 g/L adsorbed higher than that of 2 g/L dosage. In conclusion synthesized and calcined Mg-Al-LDH is capable of removing boron from aqueous solutions with small dosages such as 2 g/L, and with higher dosages higher adsorption capacity is achieved.

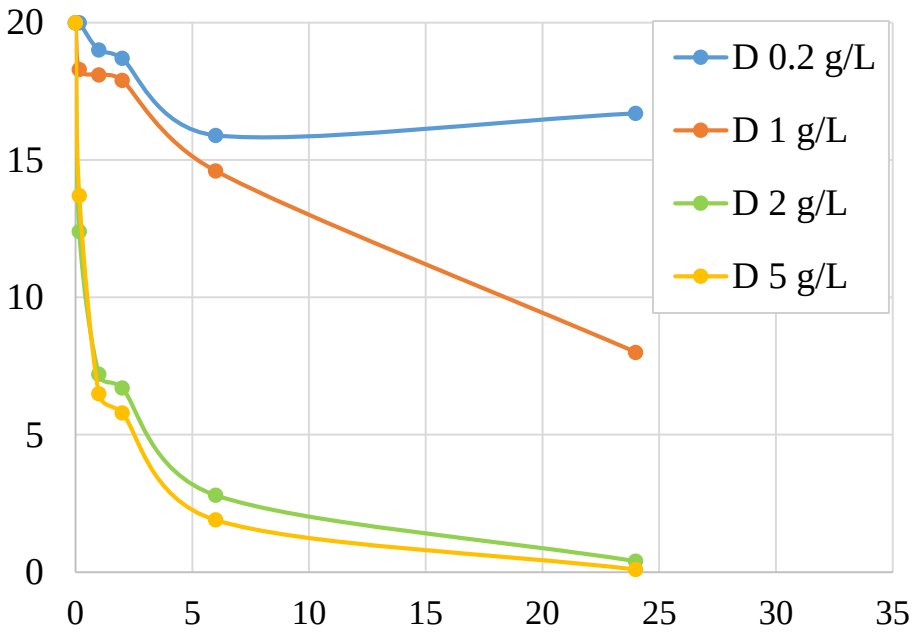

Figure 8 Dosage effect on the enhancement of boron adsorption on Mg-Al LDH, (experimental conditions: initial concentration = 20 mg/L, 25 ^{o}C and pH = 9)

3.6. Aerobic and Anaerobic Effects

In order to consider the effect of the reaction environment aerobic and anaerobic tests were conducted in the duration of 24-hour reaction time. Which were compared with anoxic data with the same basic variables, Fig .09 shows the results. The aerobic approach was the least efficient in adsorbing the contaminant. Whereas the anaerobic approach reached higher removability than the aerobic, before reaching equilibrium at boron concentration of 1.3 mg/L. Anoxic approach proved to be more efficient than the previous two methods as it is shown in the figure where by the end of reaction time the boron concentration reached 0.4 mg/L. To conclude that, adsorption of boron on Mg-Al-LDH is best achieved under anoxic conditions. Whereas, aerobic conditions which is basically pumping air into the sample batch throughout the reaction time; not only caused lesser adsorption of the contaminant, but lead to clear desorption.

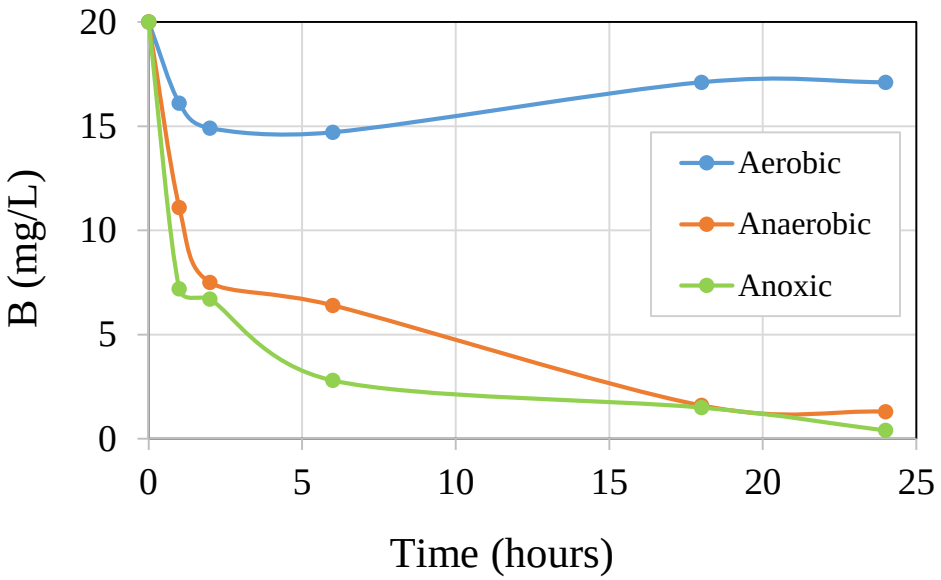

Figure 9 Aerobic, anaerobic and anoxic effect on boron adsorption on Mg-Al-LDH, (experimental conditions: initial concentration = 20 mg/L, 25 ^{o}C, pH = 9 and Mg-Al-LDH dosage of 2 g/L)

3.7. Seawater

This experiment was conducted to study the effect of applying Mg-Al-LDH on synthesized seawater to observe the material effect on removing boron mixed with different elements found in such waters. In Fig. 10 it is clear that sorption of boron in average seawater concentration is being interfered with the competing coexisting ions; thus, removal of the targeted contaminant is not fully detected. Consideration of the previous result, two more stocks of synthesized boron solution (synthesized seawater with increased initial boron concentration at 20 mg/L) were used to further study the sorption of the LDH at different dosages (2 and 5 g/L). Looking at the figure it is clear that with higher initial boron concentrated samples, visible sorption of targeted contaminant is achieved; that is due to having dominating boron species in regard to the competing coexisting ions in the solution to be adsorbed on to Mg-Al-LDH. In this case the 2 g/L dosage demonstrated higher removal rates than that of 5 g/L; which could be explained by two points happening simultaneously, the first would be the competition between boron and coexisting ions in the solution regardless of the dominance of boron species. The second point, is the availability of the adsorbent dosage in regard to boron initial concentration is too high, resulting in low removal of boron from the synthesized solution. In conclusion, it is clear that sorption of boron in average seawater concentration is being interfered with the competing coexisting ions, thus removal of said ions before treating for boron is required.

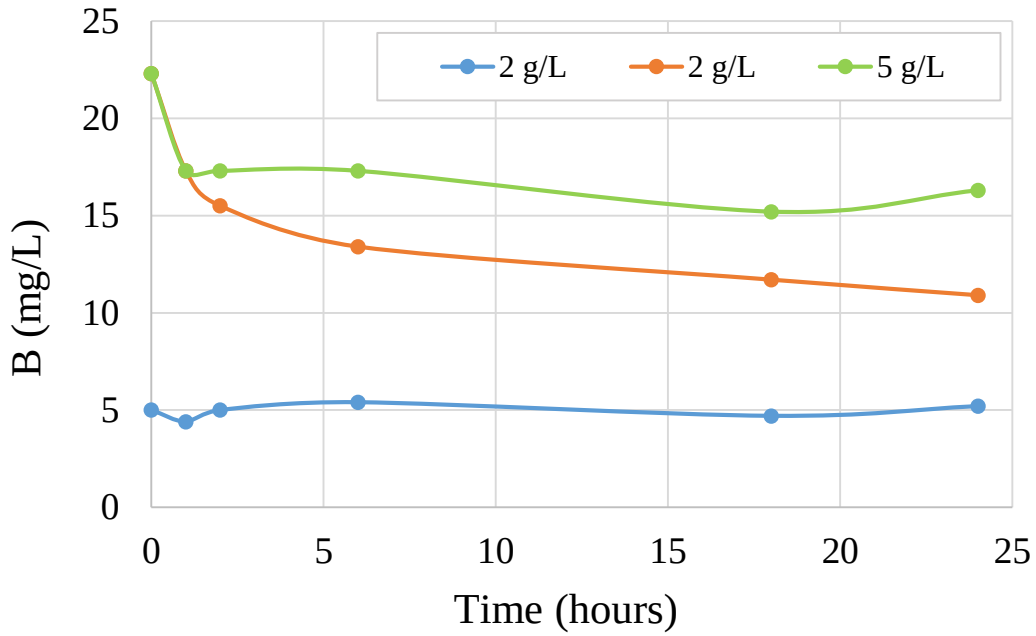

Figure 10 Adsorption of boron on Mg-Al LDH from synthesized seawater, (experimental conditions: 25 ^{o}C, pH = 9 and anoxic environment)

Samples of solid residues of the initial boron concentration of 20 mg/L batch were collected for XRD analysis in order to further analyze previously discussed results. Fig.11 shows the interference of the different existing co-ions with the adsorption of boron on Mg-Al-LDH. It is also rather different than the previously discussed XRD graph showcasing the spent solid residues of only boron contaminated solutions in Fig. 03. Potassium appears to be the most interfering ion with boron as visible in the figure corresponding to the formation of potassium borate (BK_3O_3) at 2-thetas 23.61°, and 39.1° peaks. Whereas, sodium boride (Na-B) and sodium chloride (BCl) are visible at 2-thetas 23.61°, and 32.24° respectively. Moreover, a specie of boron in the form of Carbonyltriborane is clearly visible at 2-thetas 10.89°, and 32.24°. Indicating clear adsorption of boron found in, synthesized seawater with increased initial boron concentration at 20 mg/L, onto Mg-Al-LDH, which supports the explanation of having dominating boron species in regard to the competing coexisting ions in the solution leads to be adsorbed on to Mg-Al-LDH.

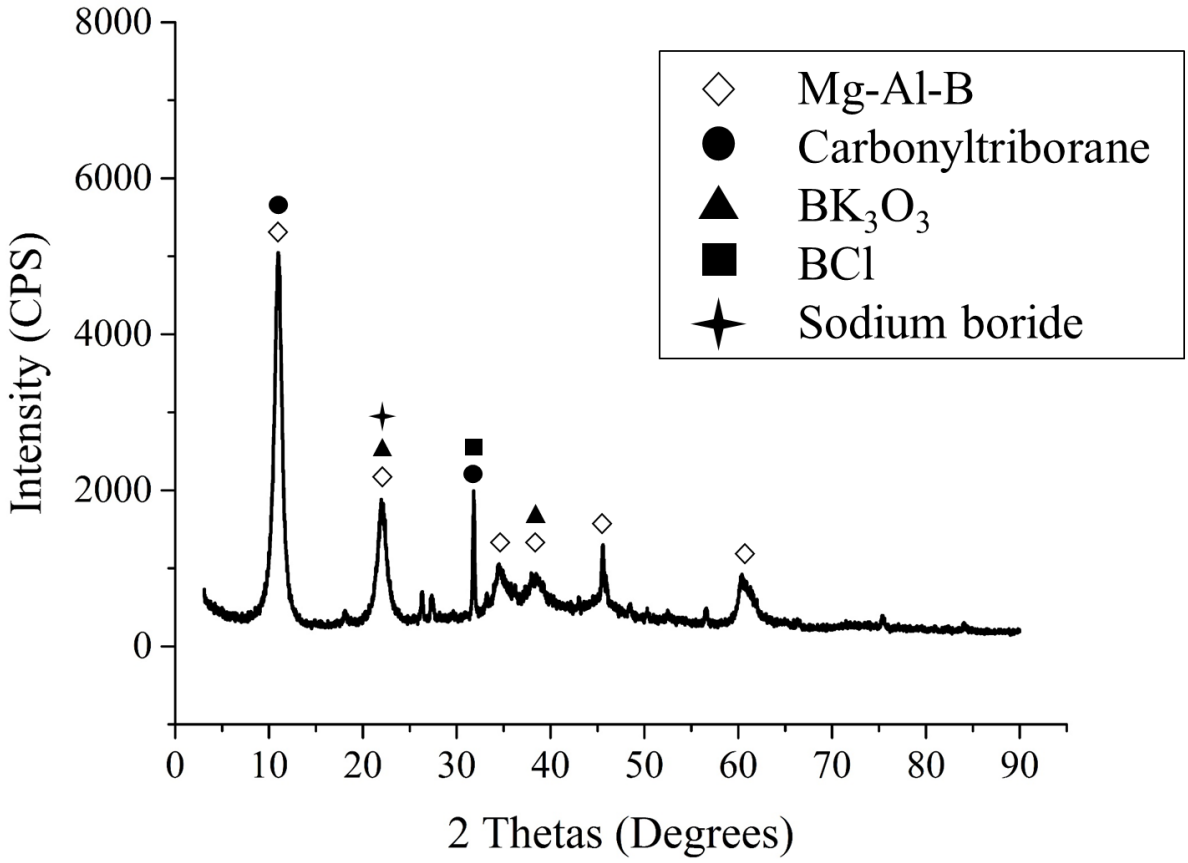

Figure 11 XRD pattern of synthesized seawater solid residuals

3.8. Mg-Al-LDH impregnated with nZVI

nZVI (Nano Zero Valant Iron) being used in many applications in water treatments it was considered to study its effects if combined with Mg-Al-LDH. Moreover, the magnetization of nZVI was also considered for an efficient way of filtration after treatment of boron contaminated waters take place. Synthesis of nZVI is conducted by following the chemical reduction method of ferric chloride precursor by sodium borohydride reductant which was previously reported [38], [39]. After synthesis of nZVI, combining it with Mg-Al-LDH was carried out in two mixing methods: physical mixing, 1:1 weight ratio of freshly synthesized nZVI and Mg-Al LDH were mixed physically. For chemical mixing, 1 g/L of Mg-Al LDH was added to a 1 g/L synthesized nZVI in deionized water and mixed for 30 minutes then separated using vacuum filter. Boron adsorption on nZVI-Mg-Al-LDH analysis results were as shown in Fig. 12. The analysis showed increased initial B-concentration after starting the experiment for both samples, then slight decrease until the 6-hour point. Only physical mixed dosage reached some removal of initially set B-concentration with boron concentration of 19.2 mg/L, then recorded desorption until the end of reaction time. Those results can be explained by discussing two points. Firstly, synthesis of nZVI require sodium borohydride which could have increased the set initial concentration. Secondly, the interference of iron particles with LDH while reaction time is commenced, or with B-reagent during the analysis.

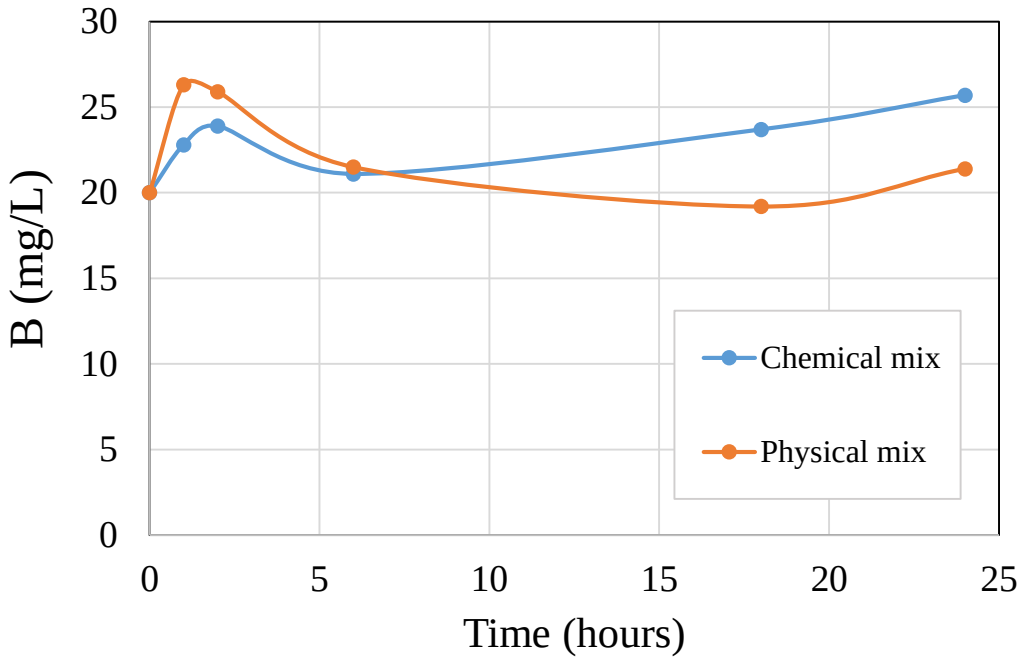

Figure 12 Results of boron adsorption on nZVI-Mg-Al-LDH, (experimental conditions: initial concentration = 20 mg/L, 25 ^{o}C, pH = 9 and Mg-Al-LDH dosage of 2 g/L)

Solid samples of freshly synthesized and mixed nZVI-Mg-Al-LDH were subjected to XRD analysis in order to further study the impregnation of nZVI onto Mg-Al-LDH as well as solid residues of spent experiments in consideration of previously discussed results. In Fig. 13, samples of physically and chemically mixed fresh nZVI-Mg-AL-LDH are displayed. The chemically mixed sample rather broad peaks which could indicate to non-crystalline mixture, unlike physically mixed sample where sharp peaks are visible. Chemically mixed sample showed Fe-Mg-Al-O complex corresponding to the peaks at 2-theats 35.2°, 44.62°, and 56.21°. On the other hand, physically mixed sample showed the same complex at 2-theats 30.12°, 35.2°, 44.62°, 57.14°, 63,2°, 73.83°, and 82.04°. Moreover, Mg-Al compound was sighted in both samples at different diffraction angels, where in chemically mixed sample at 2-thetas 35.2°, 44.62°, 46.84°, and 63.92°, and 11.4°, 24.31° in the physically mixed sample. That could indicate that both nZVI and Mg-Al-LDH were not in complete homogeneity when mixed physically as it is visible at 2-thetas 44.4° where Fe0 is sighted, which is associated to the presence of the zero valent state of iron [32], [40].

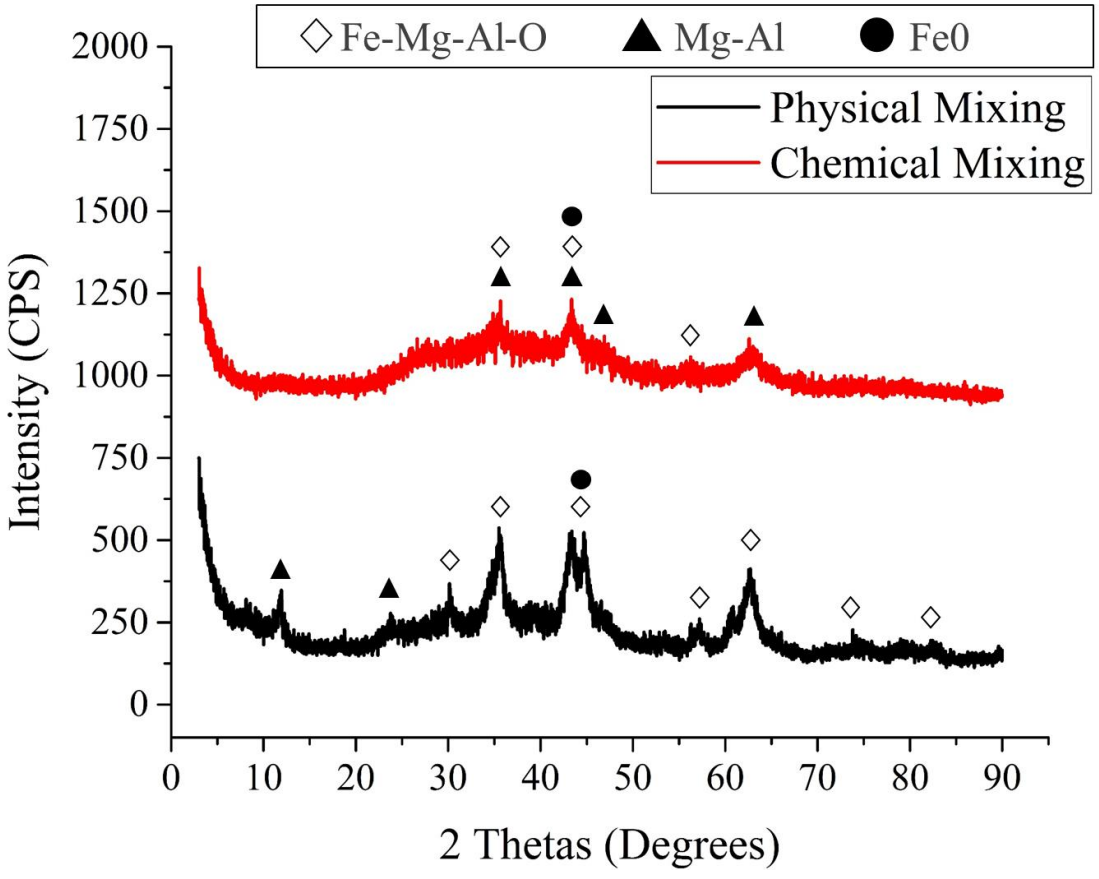

Figure 13 XRD pattern of freshly mixed nZVI-Mg-Al-LDH samples

As for the collected solid residuals from previously discussed experiment, Fig. 14 illustrates their XRD patterns. Counts of Mg-Al-B-O complex has been sighted in various peaks of both samples, corresponding to the peaks at 2-thetas 35.4°, 45.01°, and 63.83°, although it is more visible in the physically mixed sample rather than the chemically mixed one. Whereas, Fe-B-O complex was shown in both patterns in correspondence to 2-thetas 26.92°, 35.4°, and 45.01° for the chemically mixed sample, and 24.62°, 30.15°, 45.01°, and 57.2° for the physically mixed sample.

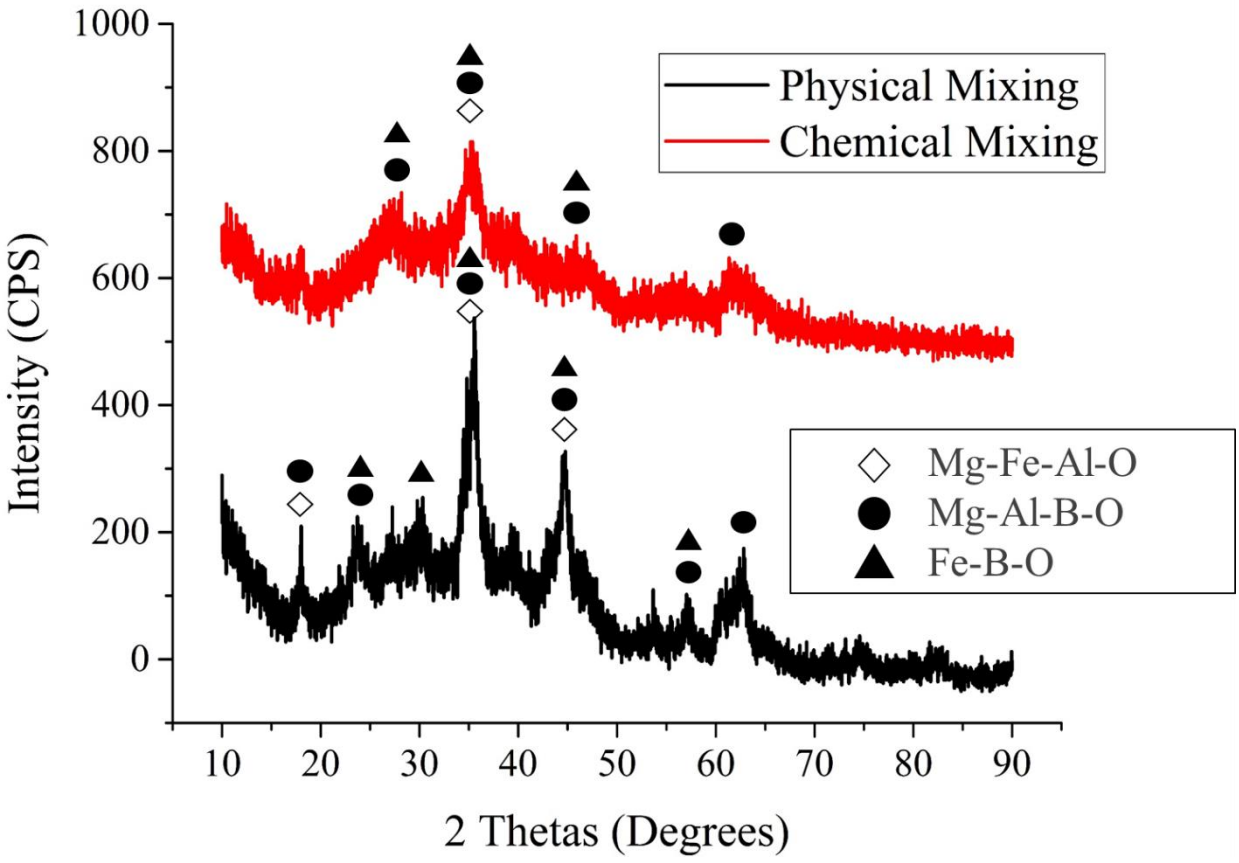

Figure 14 XRD pattern of spent nZVI-Mg-Al-LDH samples

3.9. Kinetics

Four kinetic models, pseudo first order, pseudo second order, elovich and intraparticle-diffusion, were applied in order to investigate the reaction rate and the associated kinetics parameters of boron sorption onto Mg-Al LDH. The following linear forms of the kinetic models were considered in the analysis [41]–[44]:

$$\log(q_e - q_t) = \log q_e - \frac{k_1}{2.303} t \quad (1) \quad \text{pseudo first order model}$$

$$\frac{t}{q_t} = \frac{1}{k_2 q_e^2} + \frac{1}{q_e} t \quad (2) \quad \text{pseudo second order model}$$

$$q_t = \frac{1}{b} \ln(ab) + \frac{1}{b} \ln t \quad (3) \quad \text{elovich model}$$

$$q_t = k_i t^{1/2} + C_i \quad (4) \quad \text{intraparticle-diffusion model}$$

Where, q_e (mg/g) is boron sorption capacity at equilibrium, q_t (mg/g) is sorption capacity at time t (min), k_1 (min^{-1}) is pseudo first order rate constant, k_2 (g/mg min) is pseudo second order rate constant, b (mg/g min) is initial sorption rate constant, a (g/mg) is elovich rate constant, k_i (mg/g min$^{1/2}$) is intraparticle-diffusion rate constant, and C_i (mg/g) is boundary layer thickness constant.

Kinetic parameters, estimated from the slope and intersection values from the linear plots, and correlation coefficients (R^2) are shown in Table 2. Results showed that the best fitting kinetic model to describe boron sorption by Mg-Al LDH is pseudo second order model corresponding to the highest correlation coefficients comparing to the other applied models. These results implied that the removal process of boron by Mg-Al-LDH is mainly governed by chemisorption interactions [45]. It was clear that the sorption kinetic rate got higher by approaching towards the neutral conditions, while it declined at the strong acidic or alkaline conditions. Moreover, the reaction rate was proportional to the increase in the temperature, reflecting the endothermic nature of the reactions as will be confirmed later by a detailed thermodynamic analysis. Furthermore, the initial concentration of boron significantly affected the kinetic rate, where the more the initial concentration, the lower the value of kinetic rate constant. Whereas, the sorption capacity at higher concentrations such as 40 and 80 mg/l depicted higher values of 18.30 and 34.60 mg/g, respectively. Additionally, the increase in the Mg-Al-LDH had a positive effect on the reaction with higher kinetic rate constant values.

				Pseudo 1st		Pseudo 2nd		Elovich			Intraparticle diffusion		
	Value	C_o (mg/l)	q_e (mg/g)	k_1 (min^{-1})	R^2	k_2 (g/mg min)	R^2	b (mg/g min)	a (g/mg)	R^2	k_i (mg/g $min^{1/2}$)	C_i (mg/g)	R^2
pH	3	20	9.85	0.00248	0.891	0.00163	**0.999**	0.7188	1.2934	0.967	0.2309	2.695	0.754
	6		9.75	0.00257	0.688	0.00215	**0.999**	0.6474	1.0351	0.856	0.2376	2.698	0.722
	9		9.90	0.00244	0.884	0.00178	**0.999**	0.8209	2.7003	0.952	0.2252	2.946	0.721
	12		6.50	0.00259	**0.988**	0.00060	**0.987**	0.7371	0.3698	0.965	0.1644	0.595	0.961
T (°C)	25	20	9.80	0.00232	0.913	0.00157	**0.997**	0.9168	4.570	0.957	0.2149	2.946	0.71
	40		9.90	0.00227	0.870	0.00234	**0.999**	1.0898	30.259	0.990	0.2117	3.424	0.642
	55		9.80	0.00204	0.736	0.00363	**0.998**	1.6805	7244.008	0.855	0.1964	3.949	0.5373
	70		9.95	0.00198	0.454	0.01317	**0.999**	1.9901	369989.53	0.729	0.1991	4.426	0.485
Initial conc. (mg/l)	5		2.49	0.00274	0.669	0.00251	**0.984**	2.0719	-0.5835	0.880	0.0690	0.220	0.836
	10		4.99	0.00203	0.524	0.04719	**1.00**	2.9449	2524.13	0.870	0.0940	2.111	0.545
	20		9.80	0.00222	0.889	0.00247	**0.998**	0.8645	3.2195	0.984	0.2150	2.593	0.772
	40		18.30	0.00231	0.945	0.00036	**0.980**	0.4432	1.6961	0.860	0.4150	2.789	0.935
	80		34.60	0.00123	0.260	0.00019	**0.781**	0.1834	1.9563	0.682	0.7239	6.136	0.549
Dosage (g)	0.02	20	33.5	0.00213	0.419	0.00014	**0.945**	0.1731	2.0316	0.677	0.7966	6.779	0.575
	0.1		12.00	0.00270	0.837	0.00014	**0.985**	0.5097	0.7517	0.736	0.3049	-0.228	0.973
	0.2		9.80	0.00238	0.920	0.00240	**0.999**	0.8435	2.8016	0.985	0.2117	2.978	0.714
	0.5		3.98	0.00238	0.880	0.00673	**0.987**	1.8685	0.8866	0.960	0.0888	1.186	0.693
Gas condition	Ae[1]	20	2.65	0.00098	0.126	0.02917	**0.832**	-65.848	_	0.001	0.0340	1.222	0.246
	An[2]		9.35	0.00254	0.970	0.00101	**0.996**	0.6874	0.7623	0.959	0.2116	2.060	0.846
	Anx[3]		9.80	0.00215	0.896	0.00188	**0.998**	0.9264	4.9575	0.964	0.2012	3.009	0.716
Solution	Seawater	5	0.30	0.00260	0.928	0.00549	**0.966**	14.779	-2.6635	0.872	0.0074	-0.001	0.852
	B[4]	20	4.55	0.00265	0.975	0.00121	**0.998**	0.9845	0.0843	0.978	0.1203	0.539	0.906
	B-0.5[5]		0.97	0.00267	0.789	0.00723	**0.964**	6.7670	-1.5158	0.714	0.0230	0.202	0.792

[1]Aerobic, [2]Anaerobic, [3]Anoxic, [4]Synthesized B-solution, and [5]Synthesized B-solution (LDH-dosage: 0.5g)

Table 2 Calculated kinetic parameters

3.10. Isotherm modeling

Three different isotherm models were applied on the boron sorption data, including Langmuir, Freundlich and Radushkevich-Dubinin (R-D) isotherm models. The following linear model formulas were considered for the isotherm analysis [46]–[49]:

$$\frac{C_e}{q_e} = \frac{C_e}{q_L} + \frac{1}{q_L k_L} \quad (5) \quad \text{Langmuir model}$$

$$\ln k_f + \frac{1}{n}\ln C_e \quad (6) \quad \text{Freundlich model}$$

$$\ln q_e = \ln q_{RD} - k_{RD}\left(RT ln\left[1 + \frac{1}{C_e}\right]\right)^2 \quad (7) \quad \text{Radushkevich-Dubinin (R-D) model}$$

Where, C_e (mg/l) is equilibrium concentration, q_L (mg/g) is maximum sorption capacity, k_L (L/mg) is Langmuir isotherm constant, k_f (L/g) is Freundlich isotherm constant, n is heterogeneity constant, q_{RD} (mg/g) is maximum R-D sorption capacity, k_{RD} (mol^2/kJ^2) is R-D isotherm constant, R (8.314 J/mol.K) is the universal gas constant, and T (K) is temperature.

Isotherm parameters were calculated from the slope and intersection values of the linear isotherm plots as shown in Fig. 15. From the presented parameters in Table 3, it was clear that Langmuir isotherm model is the best fitting model to describe the sorption data of boron with the highest correlation percentage of 99.96%. Such results suggested the uniformity of the sorption sites' energies of Mg-Al LDH [46], [47]. Moreover, it was confirmed that boron removal by Mg-Al LDH occurred through a mono-layer sorption which supported the formerly mentioned kinetic analysis results. However, Freundlich isotherm model showed a good fitting as well with heterogeneity constant (n) value of 12.447, confirming the presence of heterogeneous sorption sites on the surface of Mg-Al LDH. Moreover, the comparison between the obtained experimental data and the non-linear plots of the isotherm model confirmed the validity of Langmuir model in describing the boron sorption process with the closest sorption capacity value (22.10 mg/g) to the experimental one (21.95 mg/g).

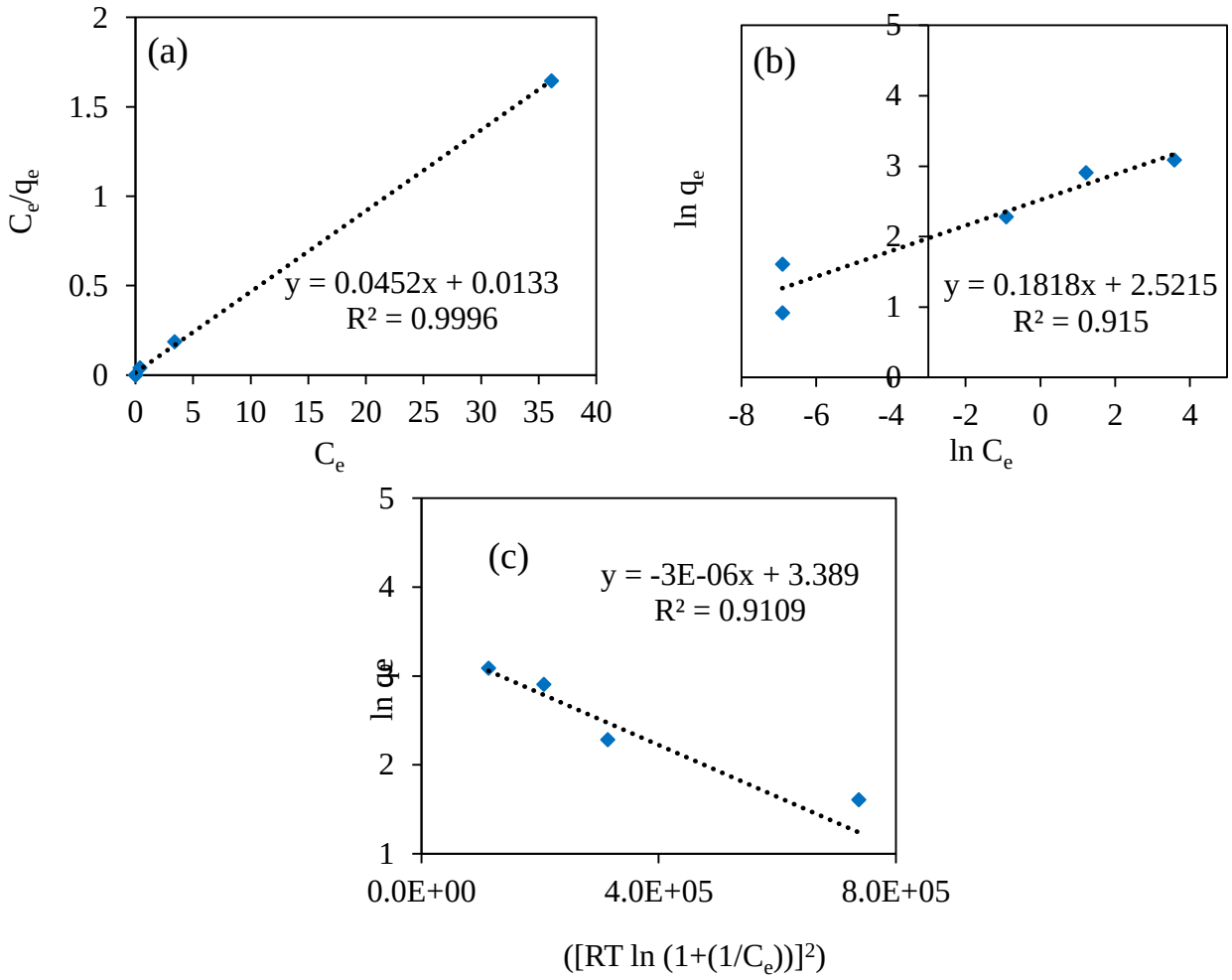

Figure 15 Linear plots of isotherm models: (a) Langmuir, (b) Freundlich, and (c) R-D

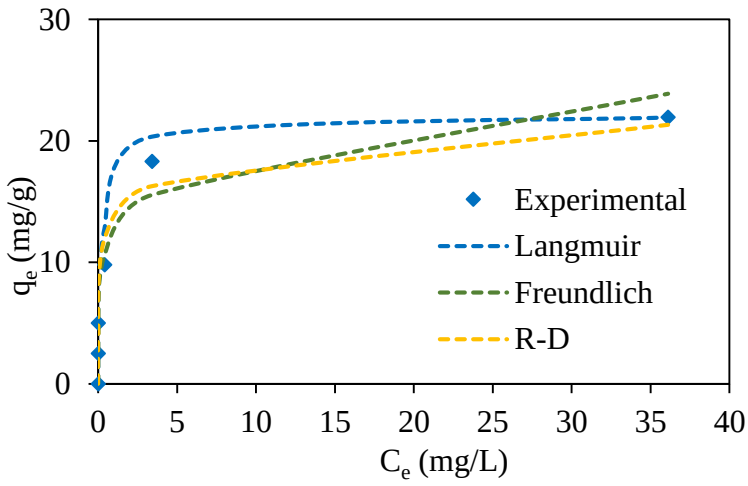

Figure 16 Non-linear plots of experimental data and isotherm models

Model	Parameter	Value
Langmuir	k_L (L/mg)	3.392
	q_L (mg/g)	22.104
	R^2	0.999
Freundlich	k_f (L/g)	5.499
	n	12.447
	R^2	0.915
R-D	k_{RD} (mol^2/kJ^2)	2.913 e^{-6}
	q_{RD} (mg/g)	29.636
	R^2	0.910

Table 3 Isotherm models' parameters

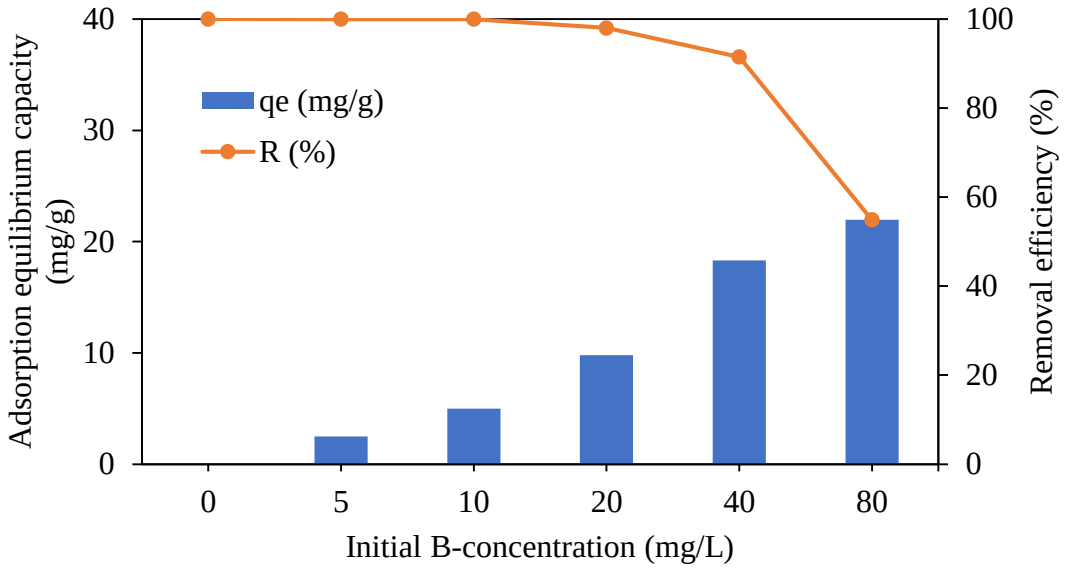

Figure 17 Sorption capacity and removal efficiency of boron onto Mg-Al LDH

Calcination showed great effect on promoting the scorpion capacity of Mg-Al-LDH towards boron, which was clearly stated in this study as shown in Table 4. Such results were in good agreement with previous reported studies confirming the enhancement influence of the calcination process. For instance, the calcined Mg-Al-LDH at 550 ºC and 450 ºC resulted in boron sorption capacities of 13 and 17.3 mg/g, respectively, while the uncalcined ones showed lower performances. For Guo et al. [50], boron to hydrotalcite ratio (B/HT= 0.5) was far greater than this study's ratio (B/HT= 0.016). Nevertheless, the presented Mg-Al-LDH in this study exhibited a comparable and almost equal boron sorption capacities for calcined and uncalcined HT, respectively. Correspondingly, the uncalcined Mg-Al-LDH removed only 37.9 mg/g of 250 mg/L initial boron concentration, considering a significantly high and impractical sorbent dosage. As shown in Fig. 17, calcined Mg-Al-LDH exhibited boron sorption capacity of around 22 mg/g corresponding to 80 mg/L initial concentration. Therefore, in terms of initial boron concentration, Mg-Al-LDH dosage and reasonable calcination

conditions the current study showed a great potential towards efficient boron removal comparing to previously reported studies.

Ref.	Materials	Conditions	Sorption capacity (mg/g)
[37]	Mg-Al LDH (calcined at 550)	IC: 100 mg/L pH: 8 D: 5 g/L	13
[31]	Mg-Al DLH (calcined at 450)	IC: 500 mg/L pH: 7 D: 5 g/L	17.3
[50]	Uncalcined Mg-Al hydrotalcite	IC: 141 mg/L D: B_I/HT= 0.5 temp: 25°C	16.47
	Calcined Mg-Al hydrotalcite		29.5
[51]	Mg/Al-LDH	IC: -- pH: 0~9 D: 2.5 g/L	14
[36]	D-LDH (calcined at 700)	IC:-- pH: 4~11 D:2.5 g/L	2.37
[30]	Uncalcined Mg-Al-LDH	IC: 250 mg/L pH: 9 D: 20 g/L	37.9
[52]	G–LDH (1.5 [gluconate]/[Mg^{2+}])	IC: 2.5mM pH: 7 D: 2.5 g/L	1.27
This study	Uncalcined Mg-Al-LDH	IC: 5 mg/L pH: 9 D: 5 g/L	16
	Calcined Mg-Al-LDH	IC: 80 mg/L pH: 9 D: 2 g/L	22.01

Table 4 Comparison between this study and other reported studies on LDH sorption capacity, where IC is boron initial concentration, and D is the sorbent dosage

3.11. Thermodynamics

Thermodynamic analysis was conducted on the adsorption data using the following equations [53]–[55]:

$$\Delta G° = -RT\ ln\ K \quad (8)$$

$$lnK = -\frac{\Delta H°}{RT} + \frac{\Delta S°}{R} \quad (9)$$

Whereas R is the Universal Gas constant (8.314 J/mol K), K is Adsorption equilibrium constant, $\Delta G°$ is change in Gibbs free energy (KJ/mol), T is temperature (Kalvin), $\Delta S°$ is change in entropy (J/mol K) and $\Delta H°$ is change in enthalpy (KJ/mol). The calculated values of these thermodynamics parameters in Table 5, were evaluated by plotting lnK vs 1/T, and knowing the slope and the interception values as displayed in Fig. 18.

Temp. °C	ΔG° (KJ/mol)	ΔH° (KJ/mol)	ΔS° (J/mol K)
25	-26.770	104.046	432.036
40	-29.948		
55	-33.287		
70	-47.961		

Table 5 Calculated thermodynamics parameters.

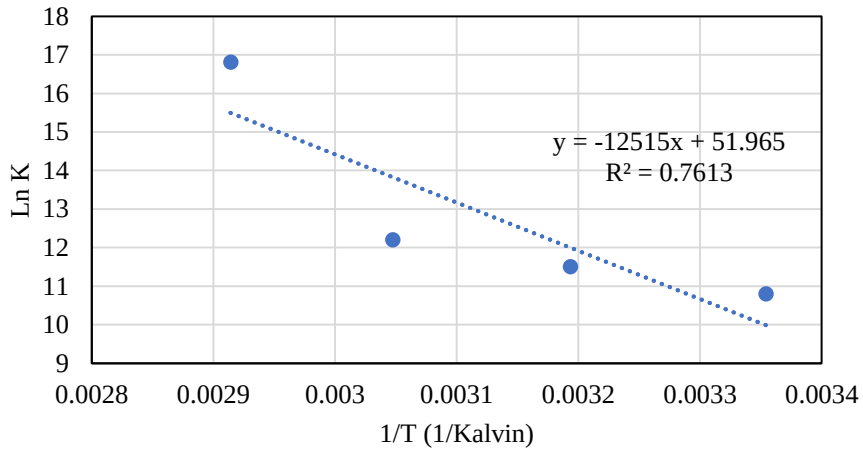

Figure 18 Linear plot of thermodynamic analysis

The negative value of $\Delta G°$ points to the endothermic nature of the removal of boron from aqueous solutions by Mg-Al-LDH indicating the enhancement in boron removal by raising the operating temperature. Moreover, the positive value of entropy change indicates that the randomness of the solid/liquid interaction increases within the adsorption process of boron. The magnitude of enthalpy change (104.04 KJ/mol) and The magnitudes of the change of the free energy indicate that boron removal by Mg-Al-LDH involves both physisorption and chemisorption processes.

3.12. Removal Mechanism

The removal of boron by the Mg-Al-LDH composite involved two possible removal mechanisms: a) sorption of the dominant boron species in the aqueous solutions on the surface of Mg-Al-LDH, which mainly conducted as anion exchange reactions, in consistence with other reported studies [51], [56]. Therefore, the boron species were captured within the interlayer of Mg-Al-LDH, as shown in Fig. 19a, through the intercalation of Mg-Al-LDH with $B(OH)_4^-$ [57]:

$$Mg - Al - LDH + B(OH)_4^- \rightarrow B(OH)_4 \cdot Mg - Al - LDH \quad (10)$$

The second involved step in the removal of boron by Mg-Al-LDH is b) the possible co-precipitation of boron species with the co-existing ions, (e.g., Na^+, Ca^{2+} and K^+) on the outer surface of the Mg-Al-LDH, which occurred in the batch experiment that was conducted using synthesized seawater. Such findings were supported by the appeared XRD peaks of that were associated to the formed precipitates (NaB_x, CaB_x and KB_x), confirming the possible competition of the co-existing ions in seawater with Mg-Al-LDH on boron removal.

The proposed removal mechanisms in this study were supported by the current kinetic analysis findings in this study, which implied that chemisorption is the main removal mechanism for boron removal by Mg-Al-LDH following the pseudo second order kinetic model. Moreover, the fitting of the sorption data with Langmuir isotherm model depicted the monolayer-capturing of boron species on Mg-Al-LDH. Moreover, the calculated adsorption free energy (E) from R-D isotherm model was 414.3 kJ/mol, within the range of 8.0-16.0 kJ/mol, confirming that the sorption process is following ion-exchange. Nevertheless, the results of thermodynamic analysis revealed the possible contribution of the physisorption in the sorption process. Such results can be interpreted by the electrostatic attraction between the negatively charged boron species and the positively charged surface of Mg-Al-LDH, which was achieved at pH values lower than the point of zero charge (PZC: pH 9.6) [37], [58], [59]. As displayed in Fig. 19b, most of the dominant boron species in aqueous solutions are presented around the neutral conditions. Therefore, electrostatic attraction between the boron species and Mg-Al-LDH were expected to be occurred at lower pH values, where Mg-Al-LDH surface was positively charged and some of boron species existed. While by raising pH value, approaching towards neutral conditions, the boron removal was induced due to the sufficiency of the variant negatively charged boron species. Whereas, at strong alkaline conditions, lower than PZC, the electrostatic repulsion resulted in less boron removal. That explanation is in a good agreement with the obtained results from pH experiments where pH 9 and pH 3 showed comparable boron removal

efficiencies, while they were much higher than that at pH 12. Hence, it should be concluded that the active pH range for boron removal by Mg-Al-LDH could be suggested from 5 to 9.6.

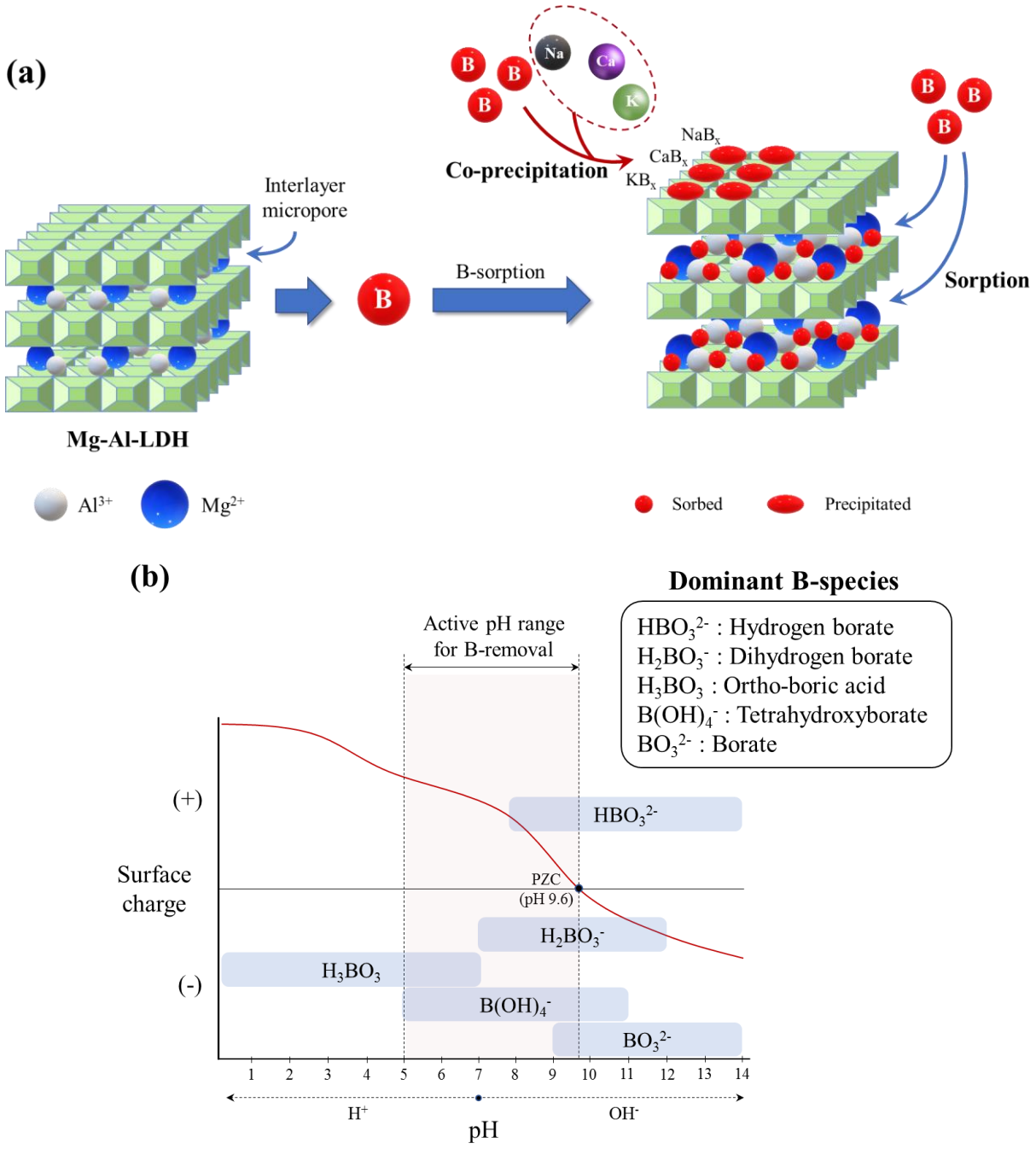

Figure 19 (a) removal mechanism of boron by Mg-Al-LDH and (b) distribution of aqueous boron species with respect to pH

4. Conclusions

Mg-Al-LDH compound was synthesized and calcined. Then, tested under various conditions to find the optimum conditions for removing of boron from aqueous solutions. The following implications were determined based on the outcomes from this study:

1) The shape of the Mg-Al-LDH sorbent can be described as micro integrated hexagonal and octahedral plate particles, and inhomogeneous particles. The sizes of those particles varied in the range of 40-100 μm. Moreover, morphology investigation revealed the particles network with a clear interlayer effect.
2) The elemental mapping revealed the well morphological distribution of Mg and Al elements, which was associated with the sorption of boron on the surface of the composite.
3) It was clear that the sorption kinetic rate got higher by approaching towards the neutral pH conditions, while it declined at the strong acidic or alkaline conditions.
4) Higher removal rates of boron in aqueous solutions were observed at increased temperatures reflecting the endothermic nature of the reaction, and at temperature 70 ℃ it reached equilibrium at less than 6 hours.
5) Synthesized and calcined Mg-Al-LDH is capable of removing high boron concentration (80 mg/L) from aqueous solutions with small dosages such as 2 g/L, with a comparable sorption capacity (22.1 mg/g) to other reported studies, and with higher dosages higher adsorption capacity is achieved.
6) Adsorption of boron on Mg-Al-LDH is best achieved under anoxic conditions. Whereas, aerobic condition which is basically pumping air into the sample batch throughout the reaction time; not only caused lesser adsorption of the contaminant, but lead to clear desorption.
7) It is clear that sorption of boron in average seawater concentration is being interfered with the competing coexisting ions, thus removal of said ions before treating for boron is required.
8) The best fitting kinetic model to describe boron sorption by Mg-Al LDH is pseudo second order model which implies that the removal process is mainly governed by chemisorption interactions. Moreover, the initial concentration of boron significantly affected the kinetic rate, where the more the initial concentration, the lower the value of kinetic rate constant. Whereas, the sorption capacity at higher concentrations such as 40 and 80 mg/l depicted higher values of 18.30 and 34.60 mg/g, respectively.
9) Isotherm modeling confirmed that boron removal by Mg-Al LDH occurred through a mono-layer sorption which supported the formerly mentioned kinetic analysis results. However, Freundlich

isotherm model showed a good fitting as well with heterogeneity constant (*n*) value of 12.447, confirming the presence of heterogeneous sorption sites on the surface of Mg-Al LDH.

10) Thermodynamic modeling revealed the positive value of entropy change indicating that the randomness of the solid/liquid interaction increases within the adsorption process of Boron. The magnitude of enthalpy change (104.04 KJ/mol) and The magnitudes of the change of the free energy indicate that boron removal by Mg-Al-LDH involves both physisorption and chemisorption processes.
11) The removal of boron by the Mg-Al-LDH composite involved two possible removal mechanisms:
    a) Sorption of the dominant boron species in the aqueous solutions on the surface of Mg-Al-LDH.
    b) The possible co-precipitation of boron species with the co-existing ions, (e.g., Na+, Ca2+ and K+) on the outer surface of the Mg-Al-LDH.
12) The proposed removal mechanisms in this study were supported by the current kinetic analysis findings in this study, which implied that chemisorption is the main removal mechanism for boron removal by Mg-Al-LDH following the pseudo second order kinetic model. Moreover, the calculated adsorption free energy (E) from R-D isotherm model was 414.3 kJ/mol, within the range of 8.0-16.0 kJ/mol, confirming that the sorption process is following ion-exchange. Nevertheless, the results of thermodynamic analysis revealed the possible contribution of the physisorption in the sorption process. Such results can be interpreted by the electrostatic attraction between the negatively charged boron species and the positively charged surface of Mg-Al-LDH, which was achieved at pH values lower than the point of zero charge (PZC: pH 9.6).
13) The core findings in the current study, considering the LDH composite and the optimized conditions, represent a vital step towards the real applications of boron removal from aqueous solutions.

5. References

[1] P. Taylor, J. L. Parks, and M. Edwards, "Critical Reviews in Environmental Science and Technology Boron in the Environment," *Crit. Rev. Environ. Sci. Technol.*, vol. 35, no. February 2013, pp. 37–41, Mar. 2007.

[2] F. S. Kot, "Boron sources, speciation and its potential impact on health," *Rev. Environ. Sci. Biotechnol.*, vol. 8, no. 1, pp. 3–28, 2009.

[3] International Atomic Energy Agency (IAEA), "Application of isotope techniques to investigate groundwater pollution," 1998.

[4] D. P, *CRC Handbook of Chemistry and Physics*, vol. 268, no. 1–3. CRC press Boca Raton, FL, 1992.

[5] D. L. Anderson, M. E. Kitto, L. McCarthy, and W. H. Zoller, "Sources and atmospheric distribution of particulate and gas-phase boron," *Atmos. Environ.*, vol. 28, no. 8, pp. 1401–1410, 1994.

[6] K. M. Al Foraij, M. K. A. El Aleem, H. Al Ajmy, and A. A. Al-Adwani, "The effect of different desalination techniques in reduction of boron content drinking water," in *IDA World Congress*, 2002, pp. 8–13.

[7] C. Paper, R. A. King, and A. City, *Survey of Boron Leve in Seawater Desalination Plants in Saudi Arabia*, no. April. 2016.

[8] A. M. Mohorjy, "Water resources management in Saudi Arabia and water reuse," *Water Int.*, vol. 13, no. 3, pp. 161–171, Jan. 1988.

[9] R. A. Al-Rasheed, S. Al-Sulami, and G. Hasan, "Survey of Boron Levels in Seawater Desalination Plants in Saudi Arabia."

[10] D. Prats, M. F. Chillon-Arias, and M. Rodriguez-Pastor, "Analysis of the influence of pH and pressure on the elimination of boron in reverse osmosis," *Desalination*, vol. 128, no. 3, pp. 269–273, 2000.

[11] E. Kir, B. Gurler, and A. Gulec, "Boron removal from aqueous solution by using plasma-modified and unmodified anion-exchange membranes," *Desalination*, vol. 267, no. 1, pp. 114–117, 2011.

[12] E. H. Ezechi, M. H. Isa, S. R. M. Kutty, and A. Yaqub, "Boron removal from produced water using electrocoagulation," *Process Saf. Environ. Prot.*, vol. 92, no. 6, pp. 509–514, 2014.

[13] E. Yoshikawa, A. Sasaki, and M. Endo, "Removal of boron from wastewater by the hydroxyapatite formation reaction using acceleration effect of ammonia," *J. Hazard. Mater.*, vol. 237–238, pp. 277–282, 2012.

[14] W. W. Chol and K. Y. Chen, “Evaluation of Boron Removal by Adsorption on Solids,” *Environ. Sci. Technol.*, vol. 13, no. 2, pp. 189–196, Feb. 1979.

[15] N. Kabay, I. Yilmaz, M. Bryjak, and M. Yüksel, “Removal of boron from aqueous solutions by a hybrid ion exchange-membrane process,” *Desalination*, vol. 198, no. 1–3, pp. 158–165, 2006.

[16] A. Q. Dr Abbas, H.Sulaymoon, Saadi, K. Al-Naseri, Ibtihal, A.Jabbar, “Boron Removal by Adsorption onto,” *J. Eng.*, vol. 19, no. February, pp. 970–977, 2011.

[17] E. Güler, C. Kaya, N. Kabay, and M. Arda, “Boron removal from seawater: State-of-the-art review,” *Desalination*, vol. 356, pp. 85–93, 2015.

[18] N. Nadav, “Boron removal from seawater reverse osmosis permeate utilizing selective ion exchange resin,” *Desalination*, vol. 124, no. 1–3, pp. 131–135, 1999.

[19] Z. Guan, J. Lv, P. Bai, and X. Guo, “Boron removal from aqueous solutions by adsorption - A review,” *Desalination*, vol. 383, pp. 29–37, 2016.

[20] G. R. Williams and D. O’Hare, “Towards understanding, control and application of layered double hydroxide chemistry,” *J. Mater. Chem.*, vol. 16, no. 30, pp. 3065–3074, 2006.

[21] D. G. Evans and X. Duan, “Preparation of layered double hydroxides and their applications as additives in polymers, as precursors to magnetic materials and in biology and medicine,” *Chem. Commun.*, no. 5, pp. 485–496, 2006.

[22] P. Dutta, S. Auerbach, and K. Carrad, *Handbook of Layered Materials*. CRC press, 2004.

[23] D. G. Evans and R. C. T. Slade, “Structural aspects of layered double hydroxides,” in *Structure and Bonding*, vol. 119, Springer, 2005, pp. 1–87.

[24] F. Zhang, X. Xiang, F. Li, and X. Duan, “Layered double hydroxides as catalytic materials: Recent development,” *Catal. Surv. from Asia*, vol. 12, no. 4, pp. 253–265, 2008.

[25] C. Taviot-Guého and F. Leroux, “In situ polymerization and intercalation of polymers in layered double hydroxides,” in *Structure and Bonding*, vol. 119, Springer, 2005, pp. 121–159.

[26] U. Costantino, V. Ambrogi, M. Nocchetti, and L. Perioli, “Hydrotalcite-like compounds: Versatile layered hosts of molecular anions with biological activity,” *Microporous Mesoporous Mater.*, vol. 107, no. 1–2, pp. 149–160, 2008.

[27] J. Liu, X. Guo, and J. Yuan, “Synthesis of Mg/Al double-layered hydroxides for boron removal,” *Desalin. Water Treat.*, vol. 52, no. 10–12, pp. 1919–1927, 2014.

[28] U. Sharma, B. Tyagi, and R. V. Jasra, “Synthesis and characterization of Mg-Al-CO3 layered double hydroxide for CO2 adsorption,” *Ind. Eng. Chem. Res.*, vol. 47, no. 23, pp. 9588–9595, 2008.

[29] T. Delazare, L. P. Ferreira, N. F. P. Ribeiro, M. M. V. M. Souza, J. C. Campos, and L. Yokoyama, “Removal of boron from oilfield wastewater via adsorption with synthetic layered double hydroxides,” *J. Environ. Sci. Heal. - Part A Toxic/Hazardous Subst. Environ. Eng.*, vol. 49, no. 8, pp. 923–932, Jul. 2014.

[30] L. Kentjono, J. C. Liu, W. C. Chang, and C. Irawan, “Removal of boron and iodine from optoelectronic wastewater using Mg-Al (NO3) layered double hydroxide,” *Desalination*, vol. 262, no. 1–3, pp. 280–283, 2010.

[31] J. Q. Jiang, Y. Xu, K. Quill, J. Simon, and K. Shettle, “Laboratory study of boron removal by Mg/Al double-layered hydroxides,” *Ind. Eng. Chem. Res.*, vol. 46, no. 13, pp. 4577–4583, 2007.

[32] I. Maamoun, O. Eljamal, A. M. E. Khalil, Y. Sugihara, and N. Matsunaga, “Phosphate Removal Through Nano-Zero-Valent Iron Permeable Reactive Barrier; Column Experiment and Reactive Solute Transport Modeling,” *Transp. Porous Media*, vol. 125, no. 2, pp. 395–412, 2018.

[33] Astm, “Standard Practice for the Preparation of Substitute Ocean Water - D 1141-93 (Reapproved 2003),” *Am. Natl. Stand.*, vol. 98, no. Reapproved 2013, pp. 98–100, 2003.

[34] Y. X. Pang and X. Bao, “Influence of temperature, ripening time and calcination on the morphology and crystallinity of hydroxyapatite nanoparticles,” *J. Eur. Ceram. Soc.*, vol. 23, no. 10, pp. 1697–1704, 2003.

[35] K. Sasaki, X. Qiu, Y. Hosomomi, S. Moriyama, and T. Hirajima, “Effect of natural dolomite calcination temperature on sorption of borate onto calcined products,” *Microporous Mesoporous Mater.*, vol. 171, pp. 1–8, 2013.

[36] X. Qiu, K. Sasaki, T. Hirajima, K. Ideta, and J. Miyawaki, “Temperature effect on the sorption of borate by a layered double hydroxide prepared using dolomite as a magnesium source,” *Chem. Eng. J.*, vol. 225, pp. 664–672, 2013.

[37] E. D. Isaacs-Paez, R. Leyva-Ramos, A. Jacobo-Azuara, J. M. Martinez-Rosales, and J. V. Flores-Cano, “Adsorption of boron on calcined AlMg layered double hydroxide from aqueous solutions. Mechanism and effect of operating conditions,” *Chem. Eng. J.*, vol. 245, pp. 248–257, 2014.

[38] R. Eljamal, O. Eljamal, A. M. E. Khalil, B. B. Saha, and N. Matsunaga, “Improvement of the chemical synthesis efficiency of nano-scale zero-valent iron particles,” *J. Environ. Chem. Eng.*, vol. 6, no. 4, pp. 4727–4735, 2018.

[39] I. Maamoun, O. Eljamal, R. Eljamal, O. Falyouna, and Y. Sugihara, “Promoting aqueous and transport characteristics of highly reactive nanoscale zero valent iron via different layered

hydroxide coatings," *Appl. Surf. Sci.*, vol. 506, p. 145018, 2020.

[40] O. Eljamal *et al.*, "Investigating the design parameters for a permeable reactive barrier consisting of nanoscale zero-valent iron and bimetallic iron/copper for phosphate removal," *J. Mol. Liq.*, p. 112144, 2019.

[41] S. K. Lagergren, "About the theory of so-called adsorption of soluble substances," *Sven. Vetenskapsakad. Handingarl*, vol. 24, pp. 1–39, 1898.

[42] C. Aharoni and D. L. Sparks, "Kinetics of soil chemical reactions—a theoretical treatment," *Rates soil Chem. Process.*, no. ratesofsoilchem, pp. 1–18, 1991.

[43] L. Deng, Y. Su, H. Su, X. Wang, and X. Zhu, "Sorption and desorption of lead (II) from wastewater by green algae Cladophora fascicularis," *J. Hazard. Mater.*, vol. 143, no. 1–2, pp. 220–225, 2007.

[44] F.-C. Wu, R.-L. Tseng, and R.-S. Juang, "Initial behavior of intraparticle diffusion model used in the description of adsorption kinetics," *Chem. Eng. J.*, vol. 153, no. 1–3, pp. 1–8, 2009.

[45] A. N. Ay, B. Zümreoglu-Karan, and A. Temel, "Boron removal by hydrotalcite-like, carbonate-free Mg-Al-NO3-LDH and a rationale on the mechanism," *Microporous Mesoporous Mater.*, vol. 98, no. 1–3, pp. 1–5, 2007.

[46] I. Langmuir, "THE ADSORPTION OF GASES ON PLANE SURFACES OF GLASS, MICA AND PLATINUM.," *J. Am. Chem. Soc.*, vol. 40, no. 9, pp. 1361–1403, Sep. 1918.

[47] D. A.O, A. Olalekan, A. Olatunya, and A. O. Dada, "Langmuir, Freundlich, Temkin and Dubinin–Radushkevich Isotherms Studies of Equilibrium Sorption of Zn 2+ Unto Phosphoric Acid Modified Rice Husk," *J. Appl. Chem.*, vol. 3, pp. 38–45, Jan. 2012.

[48] L. V Radushkevich, "Potential theory of sorption and structure of carbons," *Zhurnal Fiz. Khimii*, vol. 23, no. 12, pp. 1410–1420, 1949.

[49] M. M. Dubinin, "Modern state of the theory of volume filling of micropore adsorbents during adsorption of gases and steams on carbon adsorbents," *Zhurnal Fiz. Khimii*, vol. 39, no. 19, pp. 1305–1317, 1965.

[50] Q. Guo, Y. Zhang, Y. Cao, Y. Wang, and W. Yan, "Boron sorption from aqueous solution by hydrotalcite and its preliminary application in geothermal water deboronation," *Environ. Sci. Pollut. Res.*, vol. 20, no. 11, pp. 8210–8219, 2013.

[51] F. L. Theiss, G. A. Ayoko, and R. L. Frost, "Removal of boron species by layered double hydroxides: A review," *J. Colloid Interface Sci.*, vol. 402, pp. 114–121, 2013.

[52] X. Qiu, K. Sasaki, T. Hirajima, K. Ideta, and J. Miyawaki, "One-step synthesis of layered double hydroxide-intercalated gluconate for removal of borate," *Sep. Purif. Technol.*, vol.

123, pp. 114–123, 2014.

[53] P. S. Kumar, S. Ramalingam, S. D. Kirupha, A. Murugesan, T. Vidhyadevi, and S. Sivanesan, “Adsorption behavior of nickel (II) onto cashew nut shell: Equilibrium, thermodynamics, kinetics, mechanism and process design,” *Chem. Eng. J.*, vol. 167, no. 1, pp. 122–131, 2011.

[54] P. SenthilKumar, S. Ramalingam, R. V Abhinaya, S. D. Kirupha, T. Vidhyadevi, and S. Sivanesan, “Adsorption equilibrium, thermodynamics, kinetics, mechanism and process design of zinc (II) ions onto cashew nut shell,” *Can. J. Chem. Eng.*, vol. 90, no. 4, pp. 973–982, 2012.

[55] M. Ahmad, K. Manzoor, P. Venkatachalam, and S. Ikram, “Kinetic and thermodynamic evaluation of adsorption of Cu (II) by thiosemicarbazide chitosan,” *Int. J. Biol. Macromol.*, vol. 92, pp. 910–919, 2016.

[56] S. Moriyama, K. Sasaki, T. Hirajima, K. Ideta, and J. Miyawaki, “Sorption properties of boron on Mg-Al bimetallic oxides calcined at different temperatures,” *Sep. Purif. Technol.*, vol. 152, pp. 192–199, 2015.

[57] T. Kameda, J. Oba, and T. Yoshioka, “Use of Mg-Al oxide for boron removal from an aqueous solution in rotation: Kinetics and equilibrium studies,” *J. Environ. Manage.*, vol. 165, pp. 280–285, 2016.

[58] R. Elmoubarki *et al.*, “Ni/Fe and Mg/Fe layered double hydroxides and their calcined derivatives: Preparation, characterization and application on textile dyes removal,” *J. Mater. Res. Technol.*, vol. 6, no. 3, pp. 271–283, 2017.

[59] E. Li, L. Liao, G. Lv, Z. Li, C. Yang, and Y. Lu, “The interactions between three typical PPCPs and LDH,” *Front. Chem.*, vol. 6, no. MAR, p. 16, 2018.